VOT 72399

WIDEBAND MICROSTRIP ANTENNAS FOR CARS AND COMMERCIAL VEHICLES MODERN COMMUNICATION SYSTEM

(ANTENA JALURMIKRO BERJALUR LEBAR UNTUK SISTEM KOMUNIKASI MODEN KERETA DAN KENDERAAN KOMERSIL)

ASSOCIATE PROFESSOR Ir. Dr. WAN KHAIRUDDIN WAN ALI

RESEARCH VOT NO: 72399

Jabatan Aeronautik dan Automotif

Fakulti Kejuruteraan Mekanikal

Universiti Teknologi Malaysia.

2003

UNIVERSITI TEKNOLOGI MALAYSIA

BORANG PENGESAHAN
LAPORAN AKHIR PENYELIDIKAN

TAJUK PROJEK : WIDEBAND MICROSTRIP ANTENNA FOR CARS AND
COMMERCIAL VEHICLE MODERN COMMUNICATION SYSTEM

Saya   WAN KHAIRUDDIN BIN WAN ALI
(HURUF BESAR)

Mengaku membenarkan **Laporan Akhir Penyelidikan** ini disimpan di Perpustakaan Universiti Teknologi Malaysia dengan syarat-syarat kegunaan seperti berikut :

1. Laporan Akhir Penyelidikan ini adalah hakmilik Universiti Teknologi Malaysia.

2. Perpustakaan Universiti Teknologi Malaysia dibenarkan membuat salinan untuk tujuan rujukan sahaja.

3. Perpustakaan dibenarkan membuat penjualan salinan Laporan Akhir Penyelidikan ini bagi kategori TIDAK TERHAD.
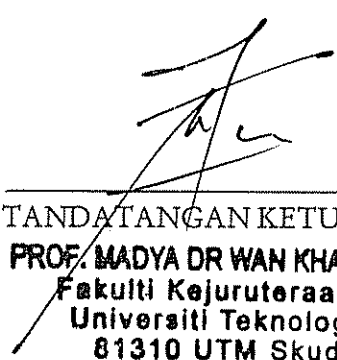
4. * Sila tandakan (/)

☐ SULIT (Mengandungi maklumat yang berdarjah keselamatan atau Kepentingan Malaysia seperti yang termaktub di dalam AKTA RAHSIA RASMI 1972).

☐ TERHAD (Mengandungi maklumat TERHAD yang telah ditentukan oleh Organisasi/badan di mana penyelidikan dijalankan).

☑ TIDAK TERHAD

TANDATANGAN KETUA PENYELIDIK

PROF. MADYA DR WAN KHAIRUDDIN WAN ALI
Fakulti Kejuruteraan Mekanikal
Universiti Teknologi Malaysia
81310 UTM Skudai, Johor
MALAYSIA

Nama & Cop Ketua Penyelidik

Tarikh :   2 4 APR 2003

CATATAN :   * Jika Laporan Akhir Penyelidikan ini SULIT atau TERHAD, sila lampirkan surat daripada pihak berkuasa/organisasi berkenaan dengan menyatakan sekali sebab dan tempoh laporan ini perlu dikelaskan sebagai SULIT dan TERHAD.

ACKNOWLEDGMENT

ABSTRACT

The basic work is directed at designing an antenna suitable for car and commercial vehicle modern communication system. One of the disadvantages of the microstrip patch antenna is its narrow bandwidth. This limitation can be overcome by modifying the conventional microstrip patch antenna. Various methods have been surveyed and this lead to the conclusion that no proper design technique has been published yet. All of the published papers and books provide the conceptual design but not the exact technical design steps. A design technique has been proposed in this project that will enhance the microstrip antenna. This technique has removed the guesswork normally associated with previous wideband microstrip patch antennas design and it consistently achieving at least 10-15% antenna bandwidth. This method involves two important design steps as follows,

a) Locating the feeding probe at a location that will give high mismatching between the feeding probe and the driven patch.

b) Using the parasitic patch of similar outer shape to tune the whole antenna structure over a wider frequency range.

The first step basically defines the location of the probe while the second step defines the function of the parasitic patch. This in effect has removed the guesswork associated with the previous design techniques.

An antenna has been designed and fabricated using the proposed technique and achieving 21% bandwidth centered at 5.441 GHz. From the point of view of electromagnetic, this antenna can be used in Industrial, Scientific and Medical (ISM) applications as well as 3G. From the point of view mechanical engineering, the antenna is very thin and can be embedded in the skin of the car thus avoiding deteriorating the existing aerodynamic properties of the host.

CONTENTS

CHAPTER	SUBJECT	PAGE

VII CONCLUSION AND SUGGESTION FOR FUTURE WORKS

CHAPTER I

INTRODUCTION

1.1   Research Background

With the proliferation of computer and wireless communication has brought about an era of wireless networking. Together with today businesses that are globally oriented, mobile communication plays a vital role in ensuring a successful business transaction.

The notion of mobile office has became a reality in today's life and for commercial vehicles, ranging from cars to large trucks and lorries, are almost all fitted with some forms of devices that allow mobile communication, be it a voice or data transmission.

With the rapid growth in multimedia technology, saw the increasing demand for a wider frequency bandwidth system than the previous one. These wider bandwidth systems require equally wider bandwidth antennas for proper functioning of the system. Several new types of antennas have been introduced in the market to cater for these needs.

For application in cars and commercial or any land based vehicle, it is common to see whip or some form of protruding type of antenna being used for radios and other communication receptions. Although the whip antennas in general are sufficient electronically for receiving electromagnetic wave, they are inefficient aerodynamically.

As the antennas unfolded, they act as bluff-bodies moving through the air. This has known to increase the overall drag coefficient of the vehicle. The increase in the overall drag coefficient means a lot to a transport operator in terms of transit time and cost saving.

In a world that aiming for higher efficient and performance car, a reduction of, 10% say, drag coefficient can make a lot of different between competitors. Furthermore, the whip antennas are inherently not rigid and this limits the dynamic capability of the vehicle.

Currently the use of WLAN and GPS in cars and other vehicles for navigation and communication have increased five fold since they were first introduced in 1970's and 1980's respectively. Inherently the whip antennas are narrow band. Thus these applications need to

1

use different type of antennas instead. In 1996 – 1998 [1 –5], techniques and several antennas have been introduced that has a wide bandwidth. Most of these antennas are made of microstrip material that are easily available and at relatively cheap cost. Nevertheless they are not specifically designed for land-based vehicles.

These microstrip antennas can be made to conform to the host body, thus making it rigid and aerodynamically efficient. Combining these properties with its wide bandwidth, they are the potential answer to the modern cars and other vehicle radio communication system.

1.2   Microstrip Antenna As A Solution For The Present Problem.

A question might be asked why microstrip antennas have been selected in this research? So far microstrip antennas satisfy the first criteria for the most sought after antenna for being small in size, light weight, ease of manufacture and readily be made to conform to the body of the host object. One principal disadvantage of microstrip antenna is its narrow bandwidth of the order 1-2%. This disadvantage, however, is being steadily overcome by continuing research into methods of increasing the bandwidth. This allows this research project to concentrate on producing the widest possible impedance bandwidth using present design techniques as described below: -

1. To combine several new and existing design technique to achieve wide impedance bandwidth.

2. To investigate a new microstrip antenna configuration that will give wide impedance bandwidth with the patch contour kept simple.

3. To investigate new patch contours that will give wide impedance bandwidth.

4. To integrate all the findings in 1 – 4 into one antenna and applying it to the modern car and land based vehicle communication system with minimum or zero effect on the existing aerodynamic properties.

Since microstrip antennas are readily made to conform to the body of the host object, the aerodynamic characteristics requirements are automatically conformed.

1.3   Justifications Of Research

Although there are several antennas that can be used for wideband communication system, mostly they were not designed, in association with expected high aerodynamic efficiency and performance of moving vehicle such as cars. This is well understood since the experts in Communication Engineering and not in Mechanical Engineering designed all of the antennas. The Aerodynamic characteristics of a car were never included in the design concept. If there are some, they are expensive.

With the increasing need for mobile office together with the demand for high aerodynamic efficiency of a car or any land-based vehicle, new type of antenna that do not interfere with the aerodynamic characteristics of the car has to be found.

In Malaysia context, most of the antennas that are used were imported from oversea. This means an out flow of currency, lack of knowledge and forever dependency on the foreign knowledge. Antenna research such as this could regionalize and localized the antenna design knowledge to Malaysia. This could spur antenna industry in Malaysia and thus could save on the outflow of currency and create better understanding on the antenna design.

Research like this can provide first hand data and experiences that can be used to assist automotive electrical/electronic engineers to design and develop a better antenna.

Hence, this research is justified to provide the solution for the above problems.

1.4   Objective Of The Research

The purpose of the research work is to produce a microstrip antenna that can be further studied and applied to the car and commercial vehicle wideband communication system. The Objectives of the research are: -

    a. To design, develop and fabricate wideband microstrip antenna for possible application in cars and commercial vehicle in conjunction with wideband communication system.

    b. To test the characteristic of the fabricated antenna.

3

1.5 Layout Of Report.

Chapter two introduce reader to the basic concept, design and application of a microstrip antenna. A comprehensive literature survey on microstrip antennas is dealt with in chapter three. Analysis and synthesis methods are described in chapter four while chapter five discusses a technique established in this research to enhance the impedance bandwidth of the microstrip antenna. In chapter six presented the design of the antenna that give 20% bandwidth. Chapter seven conclude the project report together with suggestion of the future works.

CHAPTER II

MICROSTRIP ANTENNA

2.1 Introduction

In wireless communication systems, the antenna is one of the most critical components. A good antenna design can improve the overall system performance considerably. An antenna is the system component that radiates or receives electromagnetic waves. It is more or less an electromagnetic transducer that in the transmitting mode converts the guided waves from a transmission line into radiated waves and vice versa when in the receiving mode. In some applications, antennas act as directional devices that optimize and enhance the transmitted or received energy in some directions while suppressing it in others. Over the years, antennas with physically small size and wide impedance bandwidth have been much sought after for several reasons. Being small means that they require less space and lightweight. This is particularly advantageous in application such as in satellite, space exploration and mobile communication. A wide impedance bandwidth means that in some applications, the antenna does not limit the system bandwidth and hence facilitates the use of filters, amplifiers, mixers and other components which are available at low cost and off the shelf. Also in some applications, wide impedance bandwidth is a fundamental requirement such as in pulse, moving target and ground penetrating radar. One class of antenna that has physically small size is the microstrip patch antenna.

Microstrip antenna is a printed type of antenna consisting of a dielectric substrate sandwiched in between a ground plane and a patch. The concept of microstrip antenna was first proposed in 1940's, thirty years before the practical antennas were produced. Since the first practical antennas were developed in early 1970's, interest in this kind of antenna increase and in 1979 the first professional meeting on microstrip antennas was held in New

5

Mexico. The microstrip antenna is physically very simple and flat and these two reasons that create great interest in this type of antenna.

Microstrip antennas have several advantages compared to other bulky type of antennas. Some of the main advantages of microstrip antennas are that it has low fabrication cost, its lightweight, low volume, and low profile configurations that it can be made conformal, it can be easily be mounted on rockets, missiles and satellites without major modifications and arrays of these antennas can simply be produced. However, microstrip antennas have some drawbacks including narrow bandwidth, low power handling capability and low gain. But with technology advancement and extensive research into this area these problems are being gradually overcome.

In many practical designs, the advantages of microstrip antennas far outweigh their disadvantages. With continuing research and development it is expected that microstrip antennas will replace conventional antennas for most applications. Some of the notable applications for microstrip antennas are in the areas of mobile satellite communications, the Direct Broadcast Satellite (DBS) system and Global Positioning System (GPS). Microstrip antennas also found useful in non-satellite-based application such as remote sensing and medical hypothermia application.

2.2 General Description

Generally, microstrip antenna consists of a dielectric substrate panel with conducting ground plane on one side and radiating patch on the other side. The radiating patch can be design in various shapes according to the desired characteristics. Some of the shapes the have been produced such as the rectangle, the disk, the triangle and the annular ring. Illustrated in Figure 2.1 is the simplest structure of a rectangular microstrip patch antenna.
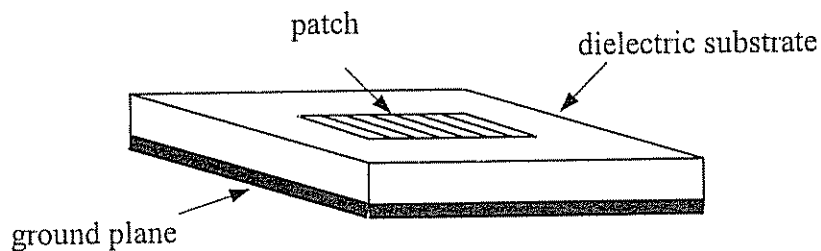
Figure 2.1 Rectangular microstrip antenna

2.2.1 Conducting Layers

The common materials used for conducting surfaces are copper foil or copper foil plated with corrosion resistant metals like gold, tin and nickel. These metals are the main choice because of their low resistivity, resistant to oxidation, solderable, and adhere well to substrate.

An alternative to metal for conducting surface is to use conductive ink. It is easier to fabricate but have three disadvantages. First, is that conductive inks cannot be soldered in the usual way, to overcome this solder pastes are used. Secondly is oxidation, but the effect is negligible since the oxide is also conductive. The third is the problem of silver ion migration. Silver ions tend to migrate under humid conditions and this will cause a short across the conductive ink lines.

2.2.2 Dielectric Substrate

In order to provide support for the patch elements dielectric substrate must be strong and able to endure high temperature during soldering process. The surface of the substrate has to be smooth to reduce losses and adhere well to the metal used. Substrate thickness and permittivity determine the electrical characteristics of the antenna. Thicker substrate will increase the bandwidth but it will cause the surface waves to propagate and spurious coupling will happen. This problem however, can be reduced or avoided by using a suitably low permittivity substrate. Below are five categories of dielectric material that are used for substrates.

(1) Ceramic – Alumina ($\varepsilon_r = 9.5$, tan $\delta = 0.0003$)

This type of dielectric has low loss but brittle. It has high frequency applications because large dimensions are not possible.

(2) Synthetic materials – Teflon ($\varepsilon_r = 2.08$, tan $\delta = 0.0004$)

7

This material possesses good electric properties but have a low melting point and have poor adhesion.

(3) Composite materials – Duroid ($\varepsilon_r = 2.2 / 6.0 / 10.8$, $\tan \delta = 0.0017$)

Composite materials are a mixture of fibreglass and the synthetic materials cited above. These materials have good electrical and physical properties.

(4) Ferrimagnetic – Ferrite ($\varepsilon_r = 9 - 16$, $\tan \delta = 0.001$)

This type of dielectric is biased by an electrical field. The resonant frequency of the antenna depends upon the biasing, hence magnetically tuneable antennas are possible.

(5) Semiconductor – Silicon ($\varepsilon_r = 11.9$, $\tan \delta = 0.0004$)

This type of dielectric can be integrated into circuit, but only small areas are available so it is not suitable for antenna applications.

2.2.3 Microstrip Feeds

There are three common techniques for exciting a particular microstrip antenna. These are coaxial probe, microstripline and aperture coupling. Matching is usually required between the antenna and the feed line, because antenna input impedances differ from customary 50ohm line impedance. Matching may be accomplished by properly selecting the location of the feed line. The location of the feed line also affects the radiation characteristics.

The coaxial probe is the most popular technique and is illustrated in Figure 2.2. The coaxial connector is attached to the ground plane and the coaxial center conductor extends through the substrate and is attached to the radiating patch. For coaxial probe the location of the feed is normally located at one third of the distance from the center of the patch to the side. The advantages of this method are that the probe location can selectively excite additional modes and it can be use with plated vias for multilayer circuits.

In the second technique, microstripline is connected directly to the radiating patch Figure 2.3. The location of the feed line may affect a small shift in resonant frequency, due to the change in coupling between the feed line and the antenna. This technique provide good

polarization however, it is very difficult to minimize the spurious radiation from the microstripline. Spurious radiation will increase sidelobes on the radiating pattern.

In the aperture coupling the feed line and the patch are on different sides of the ground plane as shown in Figure 2.4. A slot is cut in the ground plane to couple the electromagnetic to the radiating patch, thus no via connectors needed. This technique is to avoid spurious radiation escapes from the feed line and corrupt the sidelobes or polarization of the antenna.
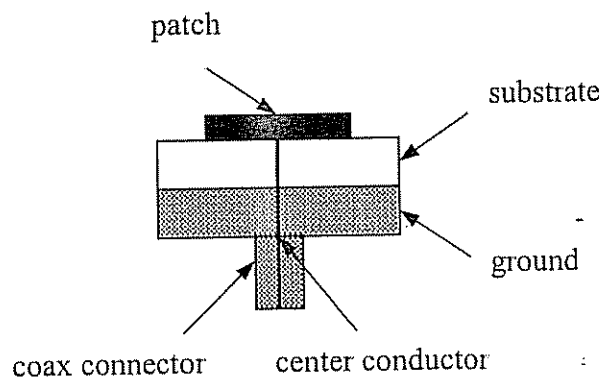
patch

substrate

ground

coax connector   center conductor

microstripline

patch

Figure 2.2 Coaxial feed
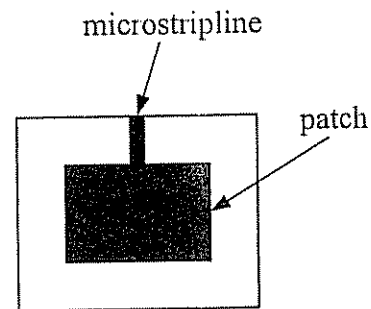
Figure 2.3 Microstrip line feed

patch   substrate

ground

slot
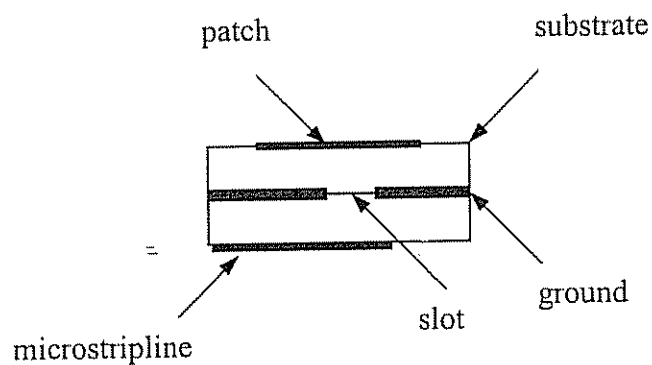
microstripline

Figure 2.4 Aperture coupling feed

2.3   Losses in Microstrip

The dissipative losses associated with microstrip lines are one of the major limitations with the microstrip antenna [1]. That is why it is important to find new ways to reduce this loss without jeopardizing the geometrical simplicity of an antenna.

There are three types of microstrip line losses; these are ohmic loss, dielectric loss and radiation loss. The ohmic loss is cause by the finite conductivity of the metal forming the circuit. The dielectric loss is a measure of the energy dissipated within the substrate. Power loss is due to radiation occurs at discontinuities in the microstrip such as open ends, splitters and impedance steps.

2.4   Commercial Applications for Microstrip Antennas

Due to reduction in manufacturing cost and the simplified design process using computer-aided design (CAD), the microstrip antenna has been increasingly in demand in the commercial sector. The current satellite communication applications benefit greatly from the compactness, lightweight and low profile of the microstrip antennas. The following section discuss briefly some of the application of microstrip antenna.

2.4.1   Mobile Satellite Communications

Mobile satellite communication can be accomplished by using either a few sets of fixed geostationary station or a larger number of low Earth-orbiting satellites. An example of the geostationary satellite systems is International Maritime Satellite System (INMARSAT), which uses frequencies in the L-band. The INMARSAT version for land application, Standard-M terminal uses a briefcase size microstrip array antenna. The antenna uses six circular patches and provides the gain of 14.5 dB. Toyota Central R&D Labs have produced

10

phased array antennas that can be steered electronically. It consist of 19 dual stacked patches to cover both transmitting and receiving frequency bands.

2.4.2 Global Positioning System (GPS)

GPS is funded by and controlled by the U. S. Department of Defense (DOD). The GPS system was originally designed for and operated by the U. S. military. The satellite-based GPS has grown to have significant commercial applications, and now there are many thousands of civil users of GPS worldwide. GPS system made of twenty-four satellites circling the Earth every twelve hours at an altitude of 20,200 km. Each satellites transmits at two frequencies in L-band, at any time four of these satellites will enable users on the ground to determine their positions every 100 nanoseconds. The GPS ground antenna has to be circularly polarized, omnidirectional, wide-beam and low gain antenna. When it comes to size, mass and cost at L-band, the microstrip patch antenna is the best candidate. Bell Corporation has produced a dual stacked patch antenna to achieve the required two L-band frequencies of the GPS system.

2.4.3 Direct Broadcast Satellite System (DBS)

A DBS system has been providing television coverage to public in many countries. The ground user antenna needs high gain of about 30dBi, circularly polarized, low axial ratio antenna and operating at the frequency of 12 GHz. Conventional parabolic reflector antennas can easily meet these specifications. However, they are rather bulky in size and cannot be installed onto an existing building. Performance of reflector antennas degraded due to rain, wind and snow. These led to development of the microstrip array antennas for DBS. For example, Yagi Antenna Corporation developed an array with 1024 circular patch elements with a peak gain of 33dBi. NHK Science and Technical Research Laboratories have developed several types of mobile DBS receiver for buses, trains, cars and airplanes. In the case of mobile DBS receivers for cars, a microstrip array antenna with a tilted beam has been investigated and tested.

2.4.4 Non-satellite Based Applications

Besides for satellite base applications microstrip antenna also used in many other areas. In aircraft, microstrip antenna has been used for the purposes of altimetry, collision avoidance and remote sensing. In medical field, microstrip antenna found to be useful for medical hyperthermia applications.

In remote sensing, the Synthetic Aperture Radar (SAR) system is used to determine ground soil grades, vegetation type, ocean wave speed and direction, agriculture usage and weather prediction. In medical area, microwave energy can be used to heat treat malignant tumors. Microstrip antenna used to apply the microwave radiation because of its lightweight and easy to handle design.

CHAPTER III

LITERATURE SURVEY

3.1   Introduction

The concept of the microstrip antenna can be traced back to the time when the printed circuits were introduced in the mid 1940's. Bruntti and Curtis [2] showed that a loop antenna can be constructed using printed circuit technique, a photograph of a loop antenna printed on a plastic sheet was presented, though no detail on the performance was given. Other sources [3 - 4] have also attributed the invention of the microstrip antenna concept to Deschamp [5] and Gutton and Baissinot [6].

In the late 1940's and during the 1950's, only a few works on microstrip antenna were reported and much of the works on microstrip were to reduce the radiation loss. No interest was shown on the potential of the microstrip as an antenna. At the beginning of the 1960's some interest was shown regarding the nature of the radiation from striplines but there was apparently little or no interest in making use of the radiation loss [7]. Other than the original papers mentioned above, no work was reported in the literature until the early 1970's.

The following is the literature survey on the subject and it is written in 2 sections, namely; 3.2 The literature survey on the general development of microstrip patch antenna, and 3.3 The literature survey on the modelling of the microstrip antenna.

3.2 Literature Survey On The General Development Of The Microstrip Patch Antennas

Bruntti and Curtis [2] presented a paper on the printed circuit techniques. The paper showed that a loop antenna can be fabricated using this technique and a photograph of a loop antenna fabricated on plastic sheet was shown. No detailed technical characteristic of the antenna was given.

Carver and Mink [3] presented a survey on microstrip antenna technology. Several theoretical analysis techniques such as the transmission line, the modal expansion (cavity) model, method of moment and the finite element method were summarised and discussed. The antenna characteristics were discussed as well as their dependence on the physical and geometrical dimensions of the patch and substrate.

Howell [8] presented an experimental data on the basic rectangular and circular microstrip patches and proposed a design procedure for both linearly and circularly polarised antennas. The gain for these antennas was between 4 to 7 dB and the operating frequencies were between the UHF and the C-band.

Derneryd [9] proposed a microstrip disc antenna operating at a theoretically calculated resonant frequency of 2.77 GHz. The antenna was found experimentally to operate at 2.44 GHz and 3.12 GHz. Impedance transformers were used to match the antenna at the resonance frequencies. It was proposed that the same technique could be applied to a different type of microstrip antenna.

Long and Walton [10] experimentally investigated two stacked circular disc with slightly different size designed for dual-frequency operation. The input impedance was measured as a function of the disc size. It was shown that when the two discs had exactly the same diameter, the antenna resonated at two frequencies separated only by 10 % apart. The bandwidth of each resonance was about 1%.

McIlvenna and Kernweis [11] carried out an investigation of the modified circular microstrip antenna element. A small single strip was used with the antenna operating at the dominant mode. It was found that by varying the length of the strip, the resonant

14

frequency and radiation pattern were altered. At one particular strip length, dual-frequency operation was achieved and by using two strips, a good pattern performance was obtained.

Schaubert, Farrar, Sindoris and Hayes [12] described a technique for controlling the operating frequency and polarisation of microstrip antennas by placing shorting posts at appropriate locations within the antenna boundaries. To make the frequency and polarisation electronically controlled, diodes were proposed to replace the shorting posts.

Chew [13] showed that for an annular ring microstrip antenna, the TM_{12} mode was the most suitable. Analysis on the resonant frequency, bandwidths, and radiation patterns in this mode was carried out.

Garg and Rao [14] experimentally investigated a microstrip antenna consisting of two different sized microstrip disc radiators. Here an impedance matching network was used for the purpose of making one feeding point for transmission or reception. The resonant frequencies were found to be shifted to 2.32 GHz. and 9.425 GHz, where else the design frequencies were 2.3 GHz and 9.25 GHz.

Ness and Young [15] investigated a microstrip antenna that produced good circular polarisation out to wide scan angle without adjustments to the ground plane. Two layers dielectric structure were used to realise optimum dielectric constant and adjusting centre frequency over a narrowband. This structure resulted in higher gain, reduction in losses and making the tolerances of the substrate less critical.

Fong, Pues and Withers [16] investigated a new feeding technique to overcome the problem associated with electrically thick microstrip patch antenna. A simple design procedure was suggested and a practical example was described.

Davidson, Long and Richards [17] carried out an experiment with a rectangular patch antenna loaded with a variable length of a short circuit coaxial stub. The result on the loaded antenna showed the existence of a dual frequency operation. The two frequencies were also found to be moving further apart from the unloaded frequency as the load approaching the edge of the radiator. A reactive load can be used to produce a dual band element having a desired frequency separation between the bands.

Davidson, Long and Richards [18] also presented a design procedure and experimental results of a dual band microstrip antenna with transmission line attached to provide

15

active loading. This technique was an improvement on the previous technique since it eliminated the need for coaxial stubs.

Mehler, Maclean and Abbas [19] suggested a mathematical model to calculate the input impedance of a coaxially fed circular microstrip disc antenna. The effect of other modes other than the dominant mode were included. A comparison study between the theoretical and experimental results were made for two values of feed pin position over the frequency range 8 GHz to 11 GHz. The result of the study was that for modes greater than of order 2, their effect were negligible.

Lee, Lee, Bobinchark [20] experimentally investigated the characteristic of a rectangular electromagnetically coupled patch antenna. The antenna consisted of a parasitic patch stacked on top of a driven patch fed by a coaxial probe. The excitation was at the resonant frequency of the TM_{01} mode, which was 10.2 GHz. E- and H-plane polar patterns, sweep frequency response and input impedance were measured and presented as a function of frequency.

Hall [21] proposed a method to tune out the probe inductance by introducing a capacitive gap on the patch surface. Using a single probe-compensated feed, it was found that there was severe radiation pattern distortion, high cross polarisation and low efficiency due to both higher order mode and surface wave. The problems were solved by using two-probe feeding.

Smith and Mayes [22] presented a method for increasing the bandwidth of microstrip antennas. Two stacked rectangular resonators were used and slots were made to couple energy between the two resonators. 4.8 % bandwidth was reported for certain cavity-backed slot antenna.

Wang, Fralich, Wu and Litva [23] suggested an aperture coupled stacked patch antenna for multi functional operation. Through careful selection of patches' dimension, either a single wideband resonance or a dual resonance behaviour was possible. A bandwidth of 20 % at 4.32 GHz. was reported.

Talty, Lee and Lee [24] experimentally investigated two layers electromagnetically coupled, circularly polarised microstrip antenna. Experimental results showed that by increasing the spacing between patches, the resonant frequency was shifted. By carefully selecting the spacing, the two-layer antenna had better axial ratio and improved directivity.

Lee and Nalbandian [25] suggested a novel dual-frequency microstrip antenna consisting of a single layer patch with the non-radiating edges connected to each other by means of a conducting foil. It was shown that the resonant frequencies can be altered by varying the length of an air gap created under the patch. Also, the input impedance can be matched by shifting the air gap without significantly altering the resonance frequencies. The radiation patterns were found to be unaffected by the modification made on the air gap.

3.3   Literature Survey Of The Modelling And Analysis Methods For The Microstrip Patch Antennas

The theoretical analysis of microstrip antenna structure started in the late 1960's. In most cases, the analyses were based on the quasi-TEM assumption which is only valid for low frequency of operation. For frequency above S-band, the technique fails to accurately predict the behaviour of the circuit. In early 1970's full-wave analysis was introduced and better analysis results were reported. The following are the surveys of the methods of modelling and analysis for microstrip antenna over the last 30 years.

Itoh and Mittra [26] presented analysis of microstrip line using the spectral domain technique. The technique made use of the Fourier transformation to reduce the complexity of the Maxwell equations. With this method, an accurate and efficient analysis for microstrip elements was possible to be carried out. The method can also be applied to microstrip antennas as indicated by the next references.

Itoh [27] presented an analysis for the microstrip resonator using spectral domain technique. Galerkin's technique (Harrinton [28]), was employed to set up a set of linear equations. The resonant frequency and quality factor were two quantities determined by this technique. The application of this technique on the microstrip antennas was presented by Itoh and Menzel in ref [32].

Munson [29] presented an experimental investigation on conformal microstrip antennas and microstrip phase array with the aim of developing an antenna suitable for missiles and spacecrafts. Experimental results from rectangular and circularly shaped microstrip

patches were presented. The experiment included a wrap-around antenna, a high gain antenna, a phase array antenna and a circularly polarised antenna.

Derneryd [30] presented an analysis on rectangular patch as two slots separated by transmission line. This approximate method was called the transmission line method and is mainly suitable for rectangular shaped patches.

Lo, Harrison, Solomon, Deschamp and Ore [31] had modelled the antenna as a cavity and solved a cavity problem. To take into account the effect of radiation, the dielectric loss tangent was increased. For thin structures, antennas having rectangular, circular, triangular and ring shapes were analysed and found to give a reasonable results.

Itoh and Menzel [32] presented a full wave analysis for open microstrip structures. The spectral domain method employed was similar to Itoh [26] but a suggestion was made that the resonant frequency must be complex in order to account for the radiation loss. Galerkin's method of moment that uses entire domain expansion function was used. The method described provided results for the resonant frequencies, radiation patterns and Q factor of various microstrip patches.

Rana and Alexopoulos [33] carried out an analysis on the microstrip dipole. The analysis follows the work by Sommerfeld [34] that involved finding the solution of the wave equation in cylindrical co-ordinates.

Pozar [35] presented the analysis on microstrip antennas taken into account the effect of feeding. Based on the electric field integral equation (EFIE) in the spectral domain, the integral which was in two dimensional plane wave form was solved via the method of moments. The relative advantages of using the entire domain and pieceswise basis function were demonstrated in this paper. Accurate results for the input impedance, mutual coupling between two patches and other parameters of the rectangular microstrip antennas were reported. The analysis also took into account the effect of the ground plane, surface wave and conductor losses.

Deshpande and Bailey [36-37] presented an analysis on microstrip antennas based on EFIE similar to Pozar [35]. Accurate results for the input impedance, mutual coupling between patches and other parameters of the rectangular microstrip patch antenna were reported.

Mosig and Gardiol [38] used the same technique as Rana and Alexopoulos [33] to analyse microstrip patch antennas.

18

Van and Van De Capelle [39] modified the transmission line method to accommodate for the mutual coupling between two patches.

Bailey and Deshpande [40] presented a detail analysis of rectangular microstrip antennas using the spectral domain method. The analysis started with deriving a dyadic Green's function that satisfies the boundary conditions for a unit current located in the plane of the microstrip patch. The Green's function was weighted with electric current density and integrated over the patch in order to calculate the radiated electromagnetic field at any point inside the dielectric. Coupled EFIE for the unknown patch current density was obtained by forcing the total tangential electric field on the patch to zero. The patch current was solved with proper selection of basis and testing function in the integral equation matrix. The current distribution on the patch was used to determine the properties of the microstrip antenna. The calculated results were compared with the measured values and given in the paper.

Lan and Sengupta [41] extended the analysis using transmission line method to include circular patch-antenna. A radial transmission line was used to model the antenna. A tunable circular patch antenna was presented in this paper.

Mosig and Gardiol [42] presented a full wave analysis for microstrip antenna based on the mixed-potential integral equation (MPIE) to solve for the current distribution and then obtain the input impedance. A rooftop subsection basis function that can be used for irregular shape patches was discussed in detail.

Araki, Ueda and Masayaki [43] carried out an analysis on circular antennas with stacked parasitic elements using the spectral domain technique in the Hankel transformation domain. The method was similar to that of Itoh and Menzel [32] in which a complex resonant frequency was calculated. In the analysis the effect of an air gap between patches was taken into account but not the effect of feeding.

Uzunoglu, Alexopoulos and Fikioris [44] presented a full wave analysis for a centre fed microstrip dipole. In this paper, the surface waves were taken into account and the input impedance was calculated using a stationary formula. An exact Green's function used was based on the two-dimensional plane waves.

Toland, Lin, Houshmand and Itoh [45] presented an application of FDTD method in simulating a three-dimensional microwave circuit containing an active and non-linear devices. A description of the procedures that were used to produce a stable large signal

19

simulation of active, non-linear circuit was given. Some results were given and a comparison was made with the measured data.

Proust, Sauviac, Amalnic and Baudrand [46] used a variational integral method in combination with Green's function and the boundary element method to characterise rectangular waveguide with electric or magnetic shield loaded by an arbitrarily shape metallic rod. The result from this study was a set of numerical basis function that was useful to model a patch antenna fed by a metallic probe. The radiation pattern and the input impedance were given.

Eswarappa and Heofer [47] studied the application of a time domain three dimensional transmission line matrix (3D-TLM) to analyse a microstrip patch antenna. To simulate the absorbing boundaries, the authors used the technique proposed by Higdon [48] and adapted it for TLM analysis of radiating structures. The study also used symmetrical condensed node (SCN) in conjunction with TLM.

Vechinski, Rao and Sarkar [49] applied the time domain integral equation method to the antennas problems. The work included a method to calculate the radiation field by an arbitrary shape three dimensional conducting antenna fed by a transient electromagnetic pulse. The mathematical solution procedure was based on the solution of integro-differential equation and using free-space Green's function which automatically enforces the radiation condition. The method of moment was employed and an iterative equation to calculate the current distribution on the structure at a certain time instant as a function of past instant plus the excitation pulse was derived. This method was known as the marching on in-time (MOT) method. The paper presented a numerical example that demonstrates the capabilities of the method.

Shively and Bailey [50] described the spectral domain analysis for imperfect conducting microstrip patch antennas by using subdomain basis functions to model the patch current density. The analysis did not include the effect of the antenna feed. The feed impedance was assumed infinite and the antenna was considered to be open circuited from the feed networks. The results presented were in the form of radar cross section as a function of frequency for a few representative cases and were compared with the measured results.

Hassani and Mirshekar-Syahkal [51] presented a paper specifically dealing with the analysis of the two layers stacked rectangular patch antenna fed by a coaxial line at

lower patch. Non-aligned, unequal patches and antennas with radome were analysed in detail. The analysis was based on solving EFIE using the spectral domain technique in conjunction with Galerkin procedure. The results of two-layer stacked rectangular antennas were given.

Chebolu, Mittral and Becker [52] presented the analysis for microstrip antenna using the finite difference time domain algorithm (FDTD). Efficient FDTD modelling and extrapolating technique were discussed in detail. The result on the performance of the techniques used were given. The paper gave an example of modelling a two-layer stacked patch array. The modelling was carried out using Sparc-10 computer with the required memory 94 Megabytes.

CHAPTER IV

ANALYSIS AND SYNTHESIS METHODS

4.1   Introduction

Mathematical modelling of the basic microstrip antenna, figure 4.1, was initially carried out using simple theory of transmission line applied to a rectangular patch fed at the centre of a radiating wall [29]. By 1978 the microstrip patch antenna was becoming much more widely known and used in a variety of communication systems [3]. This was accompanied with increased attention given by the theoretical community to improve mathematical models that could be used for design and analysis. In this chapter the author describes four most frequently used synthesis and analysis methods available and discussed the suitability of each method in the light of the present project. These methods are as follows;

1.   Transmission line model
2.   Modal-expansion cavity model
3.   Spectral domain integral equation method
4.   Finite difference time domain method.
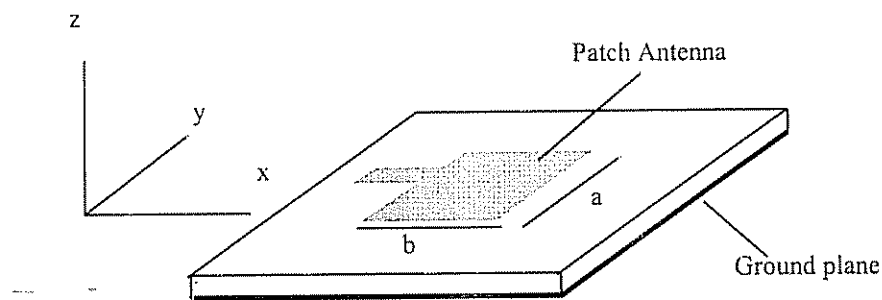
Figure 4.1 Basic microstrip patch antenna

4.2   Transmission Line Model

This method of analysis has been used for analysis in the early days of microstrip antennas. The best and the simplest example of analytical description of this method was given by Munson [29]. In order to understand this method and to be able to make useful comparison between different methods of analysis, the analytical description will be reproduced below.

Figure 4.2 Transmission-line model of rectangular microstrip

23

In Munson's [29] analytical description, the transmission line theory and model were utilised and the patch shown in figure 4.1 was modelled as two parallel radiating slots as shown in figure 4.2. Each radiating edge of length a is modelled as a narrow slot radiating into a half space with slot admittance given by
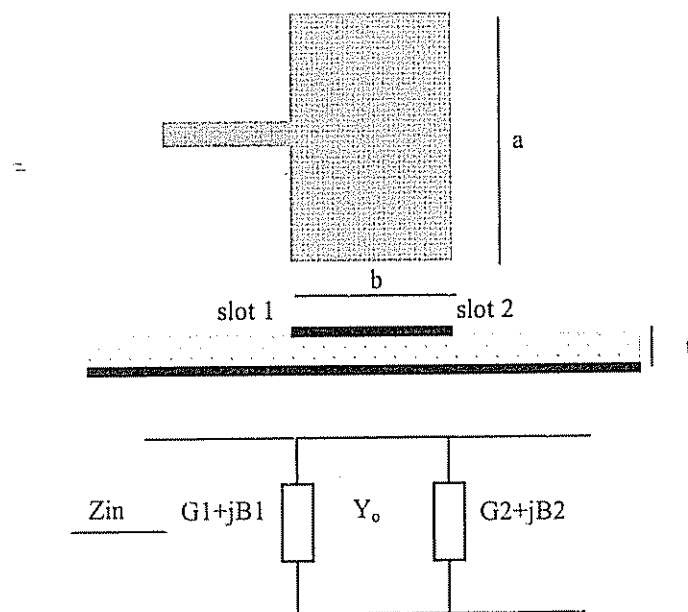
$$G1 + jB1 \approx \frac{\pi a}{\lambda_o Z_o}\left[1 + j(1 - 0.636 \ln(k_o w))\right] \qquad 4.1$$

where λ_o = free space wavelength

$$Z_o = \sqrt{\frac{\mu_o}{\varepsilon_o}} \qquad k_o = \frac{2\pi}{\lambda_0} \qquad w = t \text{ (the substrate thickness)}$$

With the assumption that no field variation along the direction parallel to the radiating edge exists, the characteristic admittance is given by

$$Y_o = \frac{a\sqrt{\varepsilon_{rd}}}{t Z_o} \qquad 4.2$$

where ε_{rd} = dielectric constant of the substrate

The normal procedure in designing rectangular patch using this method is to have each slot excited 180° out of phase to each other. Ideally this is done by choosing $b = \frac{\lambda_d}{2}$,

where $\lambda_d = \frac{\lambda_o}{\sqrt{\varepsilon_{rd}}}$. Due to the effect of fringe field, practically d is chosen slightly less

than $\frac{\lambda_d}{2}$. The admittance of slot 2 after transformation becomes,

$$G2 + jB2 = G1 - jB1$$

thus the total input admittance at resonance becomes,

$$Y_{in} = (G1 + jB1) + G2 + jB2 = 2G1 \qquad 3.4$$

4.3

The resonant frequency is found from

$$f_r = \frac{c}{\lambda_d \sqrt{\varepsilon_{rd}}} = q\frac{c}{2b\sqrt{\varepsilon_{rd}}} \qquad 4.5$$

where q = reduction factor in length of b due to fringe field effect

The model can be extended for a probe fed patch as shown in figure 4.3. Each edge admittance is calculated exactly as before and the input admittance is found by transforming both admittances through distance L1 and L2. The advantage of this model

24

lies in its simplicity, i.e. the resonant frequency and input impedance are given by simple formulas. The reduction factor q determines the accuracy of the resonant frequency and in practice is determined by measuring f_r for a rectangular patch on a given substrate. It is then assumed that the same q value holds for patches of other sizes on the same substrate and in the same general frequency range [3]. The disadvantages of using this model are that it is only useful for patches of rectangular shape, the fringe factor q must be empirically determine, it ignores field variations along the radiating edge, it is not adaptable to inclusion of the feed [3] and it is not adaptable for multi layer and multi conductor patches.
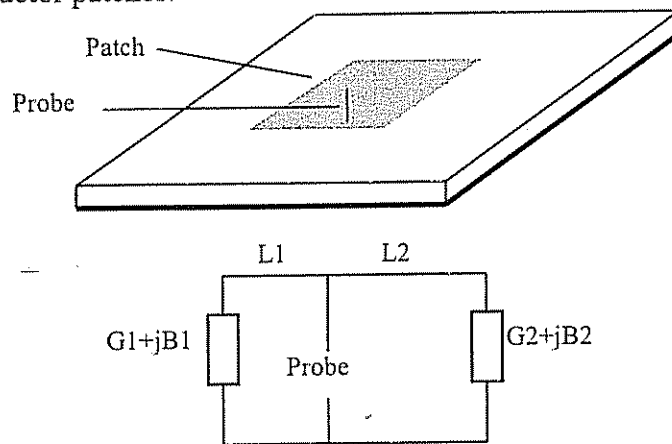
Figure 4.3 Transmission-line model of probe fed patch antenna

4.3 Modal-expansion Cavity Model

Considering the same basic microstrip patch antenna as shown in figure 4.1, for substrate height, t, much less than the operating wavelength, the electric field underneath the patch within the substrate has essentially only a z-component and the magnetic field has essentially x and y components. The tangential component of the magnetic field at the edge is very small [1]. Thus, the microstrip patch can be modelled as a cavity, bounded at its top and bottom by electric walls and on it sides by a magnetic wall. Under these conditions, the field structure within the cavity at resonance is the dual of the field structure at the cut-off frequency of a TE mode in metal waveguide

25

whose conducting boundary has the same shape as the effective boundary of the patch. Thus it is not normally necessary to analyse the field structure of this simplified model of the microstrip directly since the solution for most cases will already be available as the dual waveguide solution [1]. It is understood that with this kind of model, no power is radiated and has purely reactive input impedance of either zero or infinite value at resonance. However following the general principle of approximation as is sometimes done when characterising many conventional antennas, one may assume that the field structure in the microstrip antenna is essentially the same as that in the cavity. In 1979, using this model Lo et. al. [53] presented the field expressions for a number of patch shapes. For the patch as shown in figure 4.1, the field components underneath the patch are the dual of those of the well known rectangular waveguide transverse electric modes. That is for TM_{mn} to z modes, the fields are,

$$E_z(x,y) = \sum_m \sum_n A_{mn} e_{mn}(x,y)$$

4.6

where $\quad A_{mn}$ = mode amplitude

$e_{mn}(x,y)$ = z - directed electric mode vector.

For a non-radiating cavity with perfect magnetic walls,

$$e_{mn}(x,y) = \frac{\chi_{mn}}{\sqrt{\varepsilon_d abt}} \cos(k_n x)\cos(k_m y)$$

4.7

where $\qquad \chi_{mn} = \begin{cases} 1 & m = 0 \text{ and } n = 0 \\ \sqrt{2} & \text{either } m = 0 \text{ or } n = 0 \\ 2 & m \neq 0 \text{ and } n \neq 0 \end{cases}$

ε_d = permittivity of the substrate

The mode vectors satisfy the homogeneous wave equation, and the eigenvalues satisfy the separation equation,

$$k_{mn}^2 = \omega_{mn}^2 \mu\varepsilon_d = k_n^2 + k_m^2$$

4.8

For the non radiating cavity, $k_n = \left(\dfrac{n\pi}{a}\right)$ and $k_m = \left(\dfrac{m\pi}{b}\right)$ and resonant frequency is

given by, $\qquad f_r = \dfrac{1}{2\sqrt{\mu\varepsilon_d}} \sqrt{\left(\dfrac{n}{a}\right)^2 + \left(\dfrac{m}{b}\right)^2}$

4.9

The magnetic field mode vectors are found from Maxwell's equations as,

$$\overline{h}_{mn} = \frac{1}{j\omega\mu} \frac{\chi_{mn}}{\sqrt{\varepsilon_d}\, abt} \left[\hat{x} k_m \cos(k_n x)\sin(k_m y) - \hat{y} k_n \sin(k_n x)\cos(k_m y) \right] \qquad 4.9a$$

This equation satisfies the boundary condition $\overline{n} \times \overline{h}_{mn} = 0$ at each perimeter wall for non-radiating case. If radiation is to allowed, the eigenvalues become complex, corresponding to complex resonant frequencies, so that $|k_n|$ is slightly less than $\frac{n\pi}{a}$ and $|k_m|$ is slightly less than $\frac{m\pi}{b}$. For a small probe, its cross section is modelled as a rectangular with area equal to dxdy located at (x_p, y_p) and the probe current is Io. The coefficient of each electric mode vector is found from [3],

$$A_{mn} = jIo\sqrt{\frac{\mu t}{ab}} \frac{k\chi_{mn}}{k^2 - k_{mn}^2} G_{mn} \cos(k_m y_p)\cos(k_n x_p) \qquad 4.10$$

Where
$$G_{mn} = \frac{\sin\left(\dfrac{n\pi dx}{2a}\right)}{\dfrac{n\pi dx}{2a}} \frac{\sin\left(\dfrac{m\pi dy}{2b}\right)}{\dfrac{m\pi dy}{2b}} \qquad 4.11$$

$$k_{mn} = \widetilde{\omega}_{mn}\sqrt{\mu\varepsilon_d}$$

$\widetilde{\omega}_{mn} = $ complex resonant frequency of the mnth mode

The equation for A_{mn} is based on the orthogonality of the mode vectors. For radiation condition, the mode vectors are no longer orthogonal in the strict sense, nevertheless the error is negligible if the substrate is electrically thin [3]. For patches fed by a microstrip transmission line at y_p, dy is set to zero and dx is the feed line width as a zero-order approximation ignoring junction capacitance effects. Substituting 4.10 into 4.6 gives,

$$E_z(x,y) = jIoZ_0 k \sum_{m=0}^{\infty}\sum_{n=0}^{\infty} \frac{\psi_{mn}(x,y)\psi_{mn}(x_p, y_p)}{k^2 - k_{mn}^2} \cdot G_{mn} \qquad 4.12$$

where
$$Z_0 = \sqrt{\frac{\mu_o}{\varepsilon_o}} \qquad k = \omega\sqrt{\mu\varepsilon_d} \qquad k_{mn}^2 = k_m^2 + k_n^2$$

$$\psi_{mn}(x,y) = \frac{\chi_{mn}}{\sqrt{ab}}\cos(k_n x)\cos(k_m y) \qquad 4.13$$

$$\approx \frac{\chi_{mn}}{\sqrt{ab}}\cos\left(\frac{n\pi x}{a}\right)\cos\left(\frac{m\pi y}{b}\right)$$

The input voltage is given by,

27

$$V_{in} = - jIoZ_o kt \sum_{m=0}^{\infty} \sum_{n=0}^{\infty} \frac{\psi_{mn}^2(x_p, y_p)}{k^2 - k_{mn}^2} G \qquad 4.14$$

$$\Rightarrow \qquad Z_{in} = \frac{V_{in}}{Io} = - jZ_o kt \sum_{m=0}^{\infty} \sum_{n=0}^{\infty} \frac{\psi_{mn}^2(x_p, y_p)}{k^2 - k_{mn}^2} G \qquad 4.15$$

The complex eigenvalue k_{10} can be found from a complex transcendental eigenvalue equation that holds for thin substrates as follows [3],

$$\tan(k_{10}b) = \frac{2k_{10}\alpha_{10}}{k_{10}^2 - \alpha_{10}^2} \qquad 4.16$$

$$\alpha_{10} = j\frac{2\pi Z_o}{\lambda_o} \frac{t}{a} Y_w \qquad 4.17$$

where Y_w is the admittance of the radiating walls at $y = 0$ and $y = b$ and is given by [53 - 54],

$$Y_w = G_w + jB_w \qquad 4.18$$

$$G_w = \frac{\left(\frac{\pi}{376}\right)}{\left(\frac{a}{\lambda_o}\right)} \qquad B_w = 0.01668\left(\frac{\Delta l}{t}\right)\left(\frac{a}{\lambda_o}\right)\varepsilon_e \qquad 4.19$$

$$\frac{\Delta l}{t} = 0.412\left[\frac{\varepsilon_e + 0.3}{\varepsilon_e + 0.258}\right]\left[\frac{\frac{a}{t} + 0.262}{\frac{a}{t} + 0.813}\right] \qquad 4.20$$

$$\varepsilon_e = \frac{\varepsilon_{rd} + 1}{2} + \frac{\varepsilon_{rd} - 1}{2}\left[1 + \frac{10t}{a}\right]^{-\frac{1}{2}} \qquad 4.21$$

Once the voltage across either radiating edge is known, the far-field radiation pattern can be calculated. For V_o as the voltage across radiating edge, far field radiation is given by,

28

$$E_\theta = -\frac{jV_o k_o a e^{-jk_o r}}{\pi r} \cos(kt \cdot \cos\theta) \left[\frac{\sin\left(k_o \frac{a}{2} \cdot \sin\theta\sin\phi\right)}{k_o \frac{a}{2} \cdot \sin\theta\sin\phi} \right] \left[\cos\left(k_o \frac{b}{2} \cdot \sin\theta\sin\phi\right)\right]\cos\phi \quad \left(0 \le \theta \le \frac{\pi}{2}\right) \qquad 4.22$$

$$E_\phi = \frac{jV_o k_o a e^{-jk_o r}}{\pi r} \cos(kt \cdot \cos\theta) \left[\frac{\sin\left(k_o \frac{a}{2} \cdot \sin\theta\sin\phi\right)}{k_o \frac{a}{2} \cdot \sin\theta\sin\phi} \right] \left[\cos\left(k_o \frac{b}{2} \cdot \sin\theta\sin\phi\right)\right]\cos\phi \quad \left(0 \le \theta \le \frac{\pi}{2}\right) \qquad 4.23$$

The advantages of using this method compared to transmission line model is that it is much more accurate formulation for the input impedance, resonant frequency, etc., for both rectangular and circular patches at only a modest increase in mathematical complexity. For more complex antenna structure such as that with multi layer substrate and conductors this method will not able to handle the problem and more rigorous method such as spectrum domain and finite different time domain analysis are required.

4.4   Spectral Domain Analysis

This type of analysis starts by firstly deriving the dyadic Green's function which satisfies the boundary conditions for a unit current located in the plane of the microstrip patch [26, 27, 32, 33, 35, 36 ,37]. By weighting the Green's function with the electric current density and integrating over the patch, the radiated electromagnetic field is calculated at any point inside the dielectric. An integro-differential equation for the unknown current density is obtained by forcing the total tangential electric field on the surface of this patch to zero. Using the proper basis and testing functions for the unknown current distribution, the integro-differential equation is reduced to a matrix equation which may be solved for the patch current. the current distribution on the patch is then used to determine the properties of the microstrip antenna. Consider the rectangular patch antenna as shown in figure 4.1, and assuming that the substrate height is much less than the operating wavelength and that the time harmonic plane wave solution proportional to $e^{j\omega t}$, the Maxwell's equations in vector form are therefore,

$$\nabla \times \overline{E} = - j\omega\mu\overline{H}$$
$$\nabla \times \overline{H} = j\omega\varepsilon\overline{E}$$

Where ε and μ are the permittivity and permeability of the region concerned and the volume source terms have been dropped. To get the Green's function, consider a unit infinitesimal current source in the $\hat{x}$ direction, located at (x_o, y_o, t) as shown in figure 4.4 below, it is desired to find the resulting Ex, Ey and Ez field due to the source. The fields inside the dielectric region can be solved simultaneously for the following wave equations,

$$\nabla \times \left(\nabla \times \overline{E}\right) = -j\omega\mu_o\left(\nabla \times \overline{H}\right)$$
$$= -j\omega\mu_o\left(j\omega\varepsilon_d\overline{E}\right)$$
$$= \omega^2\mu_o\varepsilon_d\overline{E}$$
$$\Rightarrow \nabla \times \left(\nabla \times \overline{E}\right) - \omega^2\mu_o\varepsilon_d\overline{E} = 0 \qquad 4.24$$

$$\nabla \times \left(\nabla \times \overline{H}\right) = \nabla \times \left(j\omega\varepsilon_d\overline{E}\right)$$
$$= j\omega\varepsilon_d\left(\nabla \times \overline{E}\right)$$
$$= j\omega\varepsilon_d\left(-j\omega\mu_o\overline{H}\right)$$
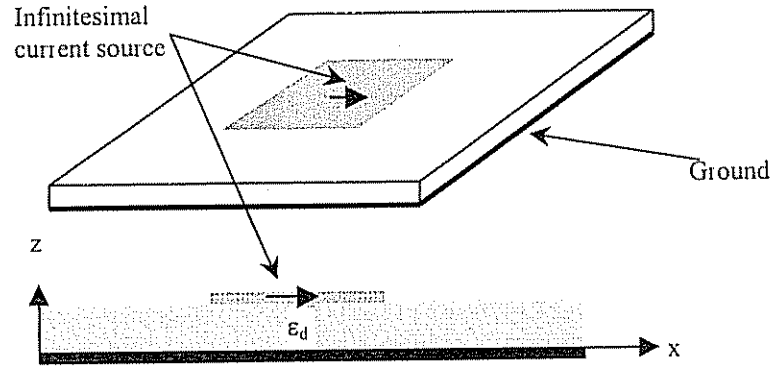$$\Rightarrow \nabla \times \left(\nabla \times \overline{H}\right) - \omega^2\varepsilon_d\mu_o\overline{H} = 0 \qquad 4.25$$

Figure 4.4 The geometry of an infinetisimal $\hat{x}$ - directed unit current element

Applying the divergence condition that $\nabla \cdot \overline{D} = 0$ to the z component of equation 4.24 yields a wave equation for Ez,

$$\frac{\partial^2 Ez}{\partial x^2} + \frac{\partial^2 Ez}{\partial y^2} + \frac{\partial^2 Ez}{\partial z^2} + \varepsilon_{rd}k_o^2 Ez = 0 \qquad 4.26$$

where $\qquad k_o = \omega\sqrt{\mu_o\varepsilon_o}$

Similarly, applying $\nabla \cdot \overline{H} = 0$ to the z component of equation 4.25 yields a wave equation for Hz given by,

$$\frac{\partial^2 Hz}{\partial x^2} + \frac{\partial^2 Hz}{\partial y^2} + \frac{\partial^2 Hz}{\partial z^2} + \varepsilon_{rd} k_o^2 Hz = 0 \qquad 4.27$$

By assuming plane wave propagation of the form $e^{\pm jk_x x} e^{\pm jk_y y} e^{\pm jk_z z}$, the dispersion relations may be obtained as,

$$k_z^2 = \varepsilon_{rd} k_o^2 - \beta^2 = k_{zd}^2 \qquad \text{in substrate region}$$

where

$$\beta^2 = k_x^2 + k_y^2 \qquad 4.28$$

The above results can be specialised to the air region ($z > d$) by allowing $\varepsilon_{rd} = 1$, in which case the propagation constant reduces to,

$$k_z^2 = k_o^2 - \beta^2 = k_{za}^2 \qquad 4.29$$

In order to satisfy the radiation conditions, the wave has to attenuate as $z \rightarrow \infty$, therefore the conditions that k_{za} in 4.29 has to be satisfied are,

$$Re[\, k_{za}\,] > 0 \qquad 4.30a$$

$$Im[\, k_{za}\,] < 0 \qquad 4.30b$$

At this stage a pair of Fourier transformation is defined as,

$$E(x, y, z) = \frac{1}{4\pi^2} \int_{-\infty}^{\infty} \int_{-\infty}^{\infty} \widetilde{E}(k_x, k_y, z) e^{jk_x x} e^{jk_y y} dk_x dk_y \qquad 4.31a$$

$$\widetilde{E}(k_x, k_y, z) = \int_{-\infty}^{\infty} \int_{-\infty}^{\infty} E(x, y, z) e^{-jk_x x} e^{-jk_y y} dx dy \qquad 4.31b$$

The reason for defining the Fourier transform pair this way is that when applied to equations 4.24 and 4.25, it will reduce them to equations involving differential with respect to only one variable. Since the Fourier transformation is associated with Fourier transform domain or spectral domain, thus this method of analysis is called spectral domain method.

Applying this Fourier transformation to equations 4.24 and 4.25, in spectral domain, the transverse field can be written in terms of $\widetilde{E}z$ and $\widetilde{H}z$ as,

31

$$\left(\varepsilon_{rd}k_o^2 + \frac{\partial^2}{\partial z^2}\right)\widetilde{E}x = jk_x\frac{\partial\widetilde{E}z}{\partial z} + \omega\mu_o k_y\widetilde{H}z \qquad\qquad 4.32$$

$$\left(\varepsilon_{rd}k_o^2 + \frac{\partial^2}{\partial z^2}\right)\widetilde{E}y = jk_y\frac{\partial\widetilde{E}z}{\partial z} - \omega\mu_o k_x\widetilde{H}z \qquad\qquad 4.33$$

$$\left(\varepsilon_{rd}k_o^2 + \frac{\partial^2}{\partial z^2}\right)\widetilde{H}x = jk_x\frac{\partial\widetilde{H}z}{\partial z} - \omega\varepsilon_o\varepsilon_{rd}k_y\widetilde{E}z \qquad\qquad 4.34$$

$$\left(\varepsilon_{rd}k_o^2 + \frac{\partial^2}{\partial z^2}\right)\widetilde{H}y = jk_y\frac{\partial\widetilde{H}z}{\partial z} + \omega\varepsilon_o\varepsilon_{rd}k_x\widetilde{E}z \qquad\qquad 4.35$$

In the above equations, $\frac{\partial^2}{\partial z^2} = -k_z^2$ and the equations can be applied for both regions, where k_z is found from either equation 4.28 or equation 4.29 depending on the region concerned. Similarly with ε_{rd} is either substrate's dielectric constant ε_{rd} or 1 if in air region. The general solutions of $\widetilde{E}z$ and $\widetilde{H}z$ are of the form,

$$\left.\begin{aligned}\widetilde{E}z &= Ae^{-jk_{za}z}\\ \widetilde{H}z &= Be^{-jk_{za}z}\end{aligned}\right\} \quad \text{for}\quad z > t\ (\text{air region}) \qquad\qquad \begin{aligned}4.36\\4.37\end{aligned}$$

$$\left.\begin{aligned}\widetilde{E}z &= C\cos(k_{zd}z) + D\sin(k_{zd}z)\\ \widetilde{H}z &= E\sin(k_{zd}z) + F\cos(k_{zd}z)\end{aligned}\right\} \quad \text{for}\quad 0 < z < t\ (\text{substrate region}) \qquad \begin{aligned}4.38\\4.39\end{aligned}$$

Applying equations 4.32 and 4.33 to equation 4.39 to enforce the boundary condition that Ex = Ey = 0 at z = 0 yield D = F = 0. There then remain four constants (A,B,C,E) to be evaluated by the continuity of Ex, Ey and Hx at z = t and a jump condition in Hy at z = t. Applying all these boundaries conditions give,

$$\widetilde{E}z = \frac{k_x k_{zd}\sin(k_{zd}t)}{j\omega\varepsilon_o Tm}e^{-jk_{za}(z-t)}e^{-jk_x x_o}e^{-jk_y y_o} \qquad\qquad 4.40$$

$$Hz = \frac{-jk_y\sin(k_{zd}t)}{Te}e^{-jk_{za}(z-t)}e^{-jk_x x_o}e^{-jk_y y_o} \qquad\qquad 4.41$$

$$\text{where}\quad Tm = \varepsilon_{rd}k_{za}\cos(k_{zd}t) + jk_{zd}\sin(k_{zd}t) \qquad\qquad 4.42$$

$$Te = k_{zd}\cos(k_{zd}t) + jk_{za}\sin(k_{zd}t) \qquad\qquad 4.43$$

The zeros of the Tm and Te functions correspond to the surface wave poles for TM and TE modes respectively. Using equations 4.32, 4.33, 4.40, 4.41 and 4.31, the transverse field at (x,y,d) can be written as,

$$Ex(x,y,d) = -\frac{jZ_o}{4\pi^2 k_o} \int\limits_{-\infty}^{\infty} \int\limits_{-\infty}^{\infty} Qxx(k_x,k_y)e^{jk_x(x-x_o)}e^{jk_y(y-y_o)}dk_x dk_y \qquad 4.44$$

$$Ey(x,y,d) = -\frac{jZ_o}{4\pi^2 k_o} \int\limits_{-\infty}^{\infty} \int\limits_{-\infty}^{\infty} Qyx(k_x,k_y)e^{jk_x(x-x_o)}e^{jk_y(y-y_o)}dk_x dk_y \qquad 4.45$$

where
$$Qxx = \frac{k_x^2 k_{za} k_{zd} \sin(k_{zd}t)}{\beta^2 Tm} + \frac{k_o^2 k_y^2 \sin(k_{zd}t)}{\beta^2 Te} \qquad 4.46$$

$$Qyx = \frac{k_x k_y k_{za} k_{zd} \sin(k_{zd}t)}{\beta^2 Tm} + \frac{k_o^2 k_x k_y \sin(k_{zd}t)}{\beta^2 Te} \qquad 4.47$$

The same analysis can be carried out to obtain the field due to y directed unit current element. This result gives,

$$Qyy = \frac{k_y^2 k_{za} k_{zd} \sin(k_{zd}t)}{\beta^2 Tm} + \frac{k_o^2 k_x^2 \sin(k_{zd}t)}{\beta^2 Te} \qquad 4.48$$

$$Qxy = Qyx \qquad 4.49$$

Equations 4.44 and 4.45 are the necessary Green's function components. To formulate the moment method solution for the usual antenna characteristic, the surface current density on the patch is expanded in a set of N expansion modes $\bar{J}_n(x,y)$ with unknown coefficients as,

$$\bar{J}(x,y) = \sum_{n=1}^{N} I_n \bar{J}_n(x,y) \qquad 4.50$$

The nth expansion mode may represent current flow in either the $\hat{x}$ or $\hat{y}$ direction. The Fourier transform of these modes is defined as,

$$F_n(k_x,k_y) = \iint\limits_{s} \bar{J}_n(x,y)e^{-jk_x x}e^{-jk_y y}dxdy \qquad 4.51$$

where s = the surface of the patch.

It is common to choose the function for $\bar{J}_n$ such that equation 4.51 is easily evaluated into closed form function. Note that since J is zero outside the patch, The Fourier transform shown in equation 4.51 is consistent with that given in equation 4.31. The electric field integral equation, which enforces the boundary conditions that the incident field from the probe plus the scattered field from the patch current must vanish on the patch surface, can then be discretized into the usual matrix form as [35]

$$[Z][I] = [V^p] \qquad 3.52$$

The impedance matrix elements are,

$$Z_{mn} = -\iint_s \bar{J}_m \cdot \tilde{E}_n \, ds = \frac{jZ_o}{4\pi^2 k_o} \int_{-\infty}^{\infty}\int_{-\infty}^{\infty} F_m^* \cdot \overline{\overline{Q}} \cdot F_n \, dk_x dk_y \qquad 4.53$$

where $\quad \tilde{E}_n$ = the electric field generated by the nth expansion mode

$\overline{\overline{Q}}$ = a dyad defined as: $\hat{x}Q_{xx}\hat{x} + \hat{x}Q_{xy}\hat{y} + \hat{y}Q_{yx}\hat{x} + \hat{y}Q_{yy}\hat{y}$

The voltage vector elements are,

$$\bar{V}_m^p = \int_s \overline{E}^p \cdot \bar{J}_m \, ds = \int_{z=0}^t \bar{J}^p \cdot \overline{E}_m \, dz$$

$$= -\frac{jZ_o}{4\pi^2 k_o} \int_{-\infty}^{\infty}\int_{-\infty}^{\infty} [Q_{zx}\hat{x} + Q_{zy}\hat{y}] \cdot F_m \, e^{jk_x x_p} e^{jk_y y_p} \, dk_x \, dk_y \qquad 4.54$$

where $\quad E^p$ = incident electric field cause by $\bar{J}^p$

$\bar{J}^p$ = unit current source on the probe.

$$Q_{zx} = \frac{jk_{za}k_x \sin(k_{zd}t)}{k_{zd}Tm} \qquad\qquad 4.55a$$

$$Q_{zy} = \frac{jk_{za}k_y \sin(k_{zd}t)}{k_{zd}Tm} \qquad\qquad 4.55b$$

Once the [Z] and [V^p] matrices have been calculated, the expansion mode coefficients can be found via equation 4.52. The input impedance is then calculated using the following formula,

$$Z_{in} = -\int_{z=0}^t E z \, dz = -[I]^T [V^p] \qquad 4.56$$

Though the spectrum domain method lacks the simplicity compared to the two previous methods discussed, it flexibility to apply to almost any shape of patch antenna is obvious. With the dramatic increase in computer capability in recent years, this method can be programmed on PC with reasonable amount of computing time. The accuracy of the solution essentially is the function of the amount of computational effort one is willing to pursue.

34

4.5   Finite Difference Time Domain Technique

This technique directly solves Maxwell's time-dependent curl equations by using central difference formula to approximate the derivatives in the curl equations. The structure under analysis is subdivided into a lattice of cubic cells where each point on the cell is assigned to represent one of the components of either the electric or magnetic field. The solution starts by assuming starting values for the field components at these points and most fields are initially set equal to zero except in the region of the source. The difference equation are time and space stepped through the lattice with previously determined fields at one point in space and at a particular instant of time being used to find the fields at adjacent points and times. Considering the same patch antenna as shown in figure 4.1, with this technique, the patch and surrounding area are divided into several FDTD cells as shown in figure 4.5. The Maxwell's equations in an isotropic medium are,

$$\frac{\partial \overline{B}}{\partial t} + \nabla \times \overline{E} = 0 \qquad\qquad 4.57$$

$$\frac{\partial \overline{D}}{\partial t} - \nabla \times \overline{H} = \overline{J} \qquad\qquad 4.58$$

$$\overline{B} = \mu \overline{H} \qquad\qquad 4.59$$

$$\overline{D} = \varepsilon \overline{E} \qquad\qquad 4.60$$

where $\overline{J}$, μ and ε are assumed to be given functions of space and time. Expanding equations 4.57 and 4.58 component-wise gives,

$$\frac{\partial B_x}{\partial t} = \frac{\partial E_y}{\partial z} - \frac{\partial E_z}{\partial y}$$

4.61

$$\frac{\partial B_y}{\partial t} = \frac{\partial E_z}{\partial x} - \frac{\partial E_x}{\partial z}$$

4.62

$$\frac{\partial B_z}{\partial t} = \frac{\partial E_x}{\partial y} - \frac{\partial E_y}{\partial x}$$

4.63

$$\frac{\partial D_x}{\partial t} = \frac{\partial H_z}{\partial y} - \frac{\partial H_y}{\partial z} + J_x$$

4.64

$$\frac{\partial D_y}{\partial t} = \frac{\partial H_x}{\partial z} - \frac{\partial H_z}{\partial x} + J_y$$

4.65

$$\frac{\partial D_z}{\partial t} = \frac{\partial H_y}{\partial x} - \frac{\partial H_x}{\partial y} + J_z$$

4.66

The grid point of the space is denoted as,

$$(i, j, k) = (i\Delta x, j\Delta y, k\Delta z)$$

4.67

and for any function of space and time, it is denoted as,

$$F(i\Delta x, j\Delta y, k\Delta z, n\Delta t) = F^n(i, j, k)$$

4.68

For perfectly conducting boundary condition and grid position as shown in figure 4.5, equation 4.61 is approximate as,

$$\frac{B_x^{n+\frac{1}{2}}\left(i, j+\frac{1}{2}, k+\frac{1}{2}\right) - B_x^{n-\frac{1}{2}}\left(i, j+\frac{1}{2}, k+\frac{1}{2}\right)}{\Delta t}$$
$$= \frac{E_y^n\left(i, j+\frac{1}{2}, k+1\right) - E_y^n\left(i, j+\frac{1}{2}, k\right)}{\Delta z}$$
$$- \frac{E_z^n\left(i, j+1, k+\frac{1}{2}\right) - E_z^n\left(i, j, k+\frac{1}{2}\right)}{\Delta y}$$
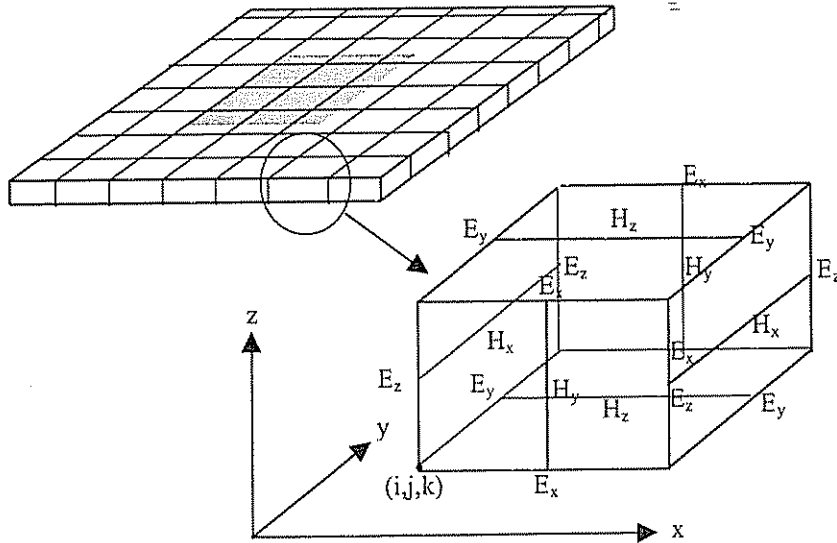
4.69

Figure 3.5 Position of various field components

36

The finite difference equations corresponding to equations 4.62 and 4.63 can be similarly constructed. For equation 4.64, the corresponding finite difference equations is,

$$
\frac{D_x^n\left(i+\frac{1}{2}, j, k\right) - D_x^{n-1}\left(i+\frac{1}{2}, j, k\right)}{\Delta t}
$$
$$
= \frac{H_z^{n-\frac{1}{2}}\left(i+\frac{1}{2}, j+\frac{1}{2}, k\right) - H_z^{n-\frac{1}{2}}\left(i+\frac{1}{2}, j-\frac{1}{2}, k\right)}{\Delta y} \qquad 4.70
$$
$$
- \frac{H_y^{n-\frac{1}{2}}\left(i+\frac{1}{2}, j, k+\frac{1}{2}\right) - H_y^{n-\frac{1}{2}}\left(i+\frac{1}{2}, j, k-\frac{1}{2}\right)}{\Delta z} + J_x^{n-\frac{1}{2}}\left(i+\frac{1}{2}, j, k\right)
$$

The finite difference equations corresponding to equations 4.65 and 4.66 can be similarly constructed. The boundary condition appropriate for the perfectly conducting surface is that the tangential component of the electric field vanishes. This condition also implies that the normal component of magnetic field vanishes on the surface. In order to start the calculation, an initial stimulus has to be applied to the system. This can be done by choosing the appropriate time dependent function of current density J. For a probe fed patch antenna on a thin substrate, J can be approximated as $J = \hat{z} A(z)f(t)\delta(x-x_p)\delta(y-y_p)$ located at the appropriate surfaces of the unit cell. To ensure computational stability, the grid size has to be chosen according to the following formula [55],

$$
\sqrt{(\Delta x)^2 + (\Delta y)^2 + (\Delta z)^2} > c \cdot \Delta t \qquad 4.71
$$

Where c is the velocity of light in the region concerned. This requirement puts a restriction on the value of Δt for a particular set of chosen values of Δx, Δy and Δz. Once the computation reach steady state, the input impedance can be evaluate from $J(i_p, j_p, k_p)$ and $E_z(i_p, j_p, k_p)$, where i_p, j_p and k_p are the x, y and z location of the probe respectively. Although this method is direct and simple in approach, the requirement for computational stability and that the grid size must be small enough so that over one increment the electromagnetic field does not change significantly, makes it difficult to apply on personnal computer PC base computation. G.S. Hilton et. al. [56] demonstrate that for a patch antenna with area of 160mm × 101mm, this methods requires 62 × 76 unit cells with a total of 60000 iteration performed. Chebolu,S. and Mittra, R. [57] reported that using more efficient analysis technique, some saving in computational random access memory (ram) and time can be achieved. Nevertheless this does not help improving the computational memory and time requirement to the extend that it can be

used on PC. The example given in reference [57] shows that for a similar patch antenna as in figure 4.1, the ram required is 94 mega-byte and the time taken is 18 hours using SPARC-10 workstation.

4.6   The Selection Of Analysis And Synthesis Method

From the discussion of the analysis methods given above, it is clear that for a simple patch antenna, i.e. single layer substrate and simple patch geometry, the transmission line model and modal expansion cavity model are the most appropriate to be used. While rigorous methods are more complete in that they offer an accurate radiation model, surface wave effect and the field internal to the patch, they are quite complicated and can not be readily implemented especially for design work. Sainati, R.A.[58] shows that the accuracy of the rigorous approaches may not be much better that the simpler transmission line and cavity models provided the latter are used within their range of validity (i.e. electrically thin substrate). In this project, a method of extending the application of cavity model in multi layer substrate is proposed and will be dealt in detail in the next chapters. When the antenna structure involves multi conductor and multi layer substrate, rigorous type of analysis must be used and the most appropriate method for PC based computation is the spectral domain analysis. It combines the needs for accuracy and computational efficiency in such a way that another rigorous method such as FDTD does not have.

CHAPTER V

BANDWIDTH ENHANCEMENT TECHNIQUES

5.1   Introduction

The bandwidth of an antenna is defined [4] as the range of frequencies within which the performance of the antenna, with respect to some characteristics, conforms to a specific standard. If this characteristic is the input impedance of the antenna, then it is well known that one of the particular characteristics of the microstrip antenna is its inherent narrow bandwidth. It was reported that the bandwidth of an antenna depends on the patch shape, the resonant frequency, the dielectric constant and thickness of the substrate [58]. Over the years, a considerable amount of research work has been carried out to enhance the antenna bandwidth and many designs have been suggested and implemented in practice. However, these designs have disadvantages related to the size, height or overall volume of the single element and the improvement in bandwidth suffers usually from a degradation of other characteristics. For a single element operating at the fundamental lowest mode, the typical bandwidth is from less than one percent to several percent for thin substrates. With the original patch antenna as shown in figure 3.1, Sanchez-Hernandez and Robertson [58] reported that there were three methods that can be employed to increase the bandwidth. The first method would be to simply increase the thickness of the substrate. The problem associated with this method is that a thicker substrate will support surface waves, which will deteriorate the radiation patterns as well as reduce the radiation efficiency. Also, as the thickness of the substrate increases, the problem associated with the feeding of the antenna arise. Additionally, high order cavity modes with the field depending on z-direction may develop,

introducing further distortion in the radiation pattern and impedance. The second technique to increase bandwidth is decreasing the relative permittivity, which has an evident limitation based on size since, for a particular frequency of operation, decreasing the relative permittivity will require an increase in the actual size of the patch. The third method is the use of a wideband matching network. The impedance matching technique was first proposed by Cralin [59] followed by the real frequency matching technique [60] and the simplified real frequency technique [61]. Such a method suffers from the inherent complexity of the network used. This chapter discusses the main techniques that have been used in practice to enhance the bandwidth of the microstrip patch antennas, either by obtaining a wider bandwidth or performing a dual-band operation or operating at lower frequency for a smaller patch.

5.2 Multi-layer Structure Antenna (Stacking Technique) [62 - 68]

One of the first published methods to enhance the antenna bandwidth is by stacking two antenna elements on top of each other. The antenna was constructed by stacking two circular elements, feeding the top patch by a coaxial connector through the ground plane as shown in figure 5.1
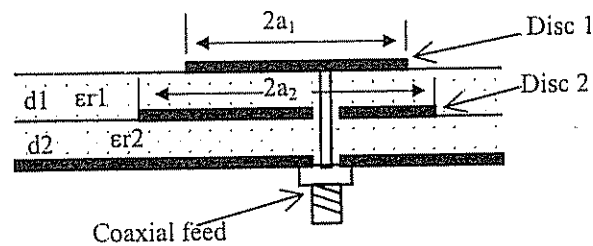

Figure 5.1 A stacked circular disc antenna

Two distinct resonant frequencies were reported, with the lower frequency was relatively steady over a range of different diameters for the upper conductor, where as the second resonant frequency was highly dependent on the radius of the two patches. Over the years, many theoretical studies have been published on this antenna structure as well as experimental results with bandwidth up to 26 % of the centre frequency f_o (VSWR < 2). A larger bandwidth may be achieved by varying the value of the two

40

heights and adjusting ε_{r2}. A recent study on a similar antenna structure includes off setting the position, varying the size and shape of the elements. However, none of the papers published thus far provide some form of practical engineering design procedure so that the antenna published can be repeated for different frequency ranges.

5.3   Microstrip Antenna With An Airgap [69 - 72]

The geometry of a microstrip patch antenna with an airgap is shown in figure 5.2. It consists of two layers, one is a substrate of thickness t and the other is an air region of thickness Δ. The effective permittivity is evidently reduced, tending toward the free space value ε_0 as the air thickness increases. This concept was also applied to the stacked patches, performing a tunable arrangement with two stacked element as shown in figure 5.3 and figure 5.4.
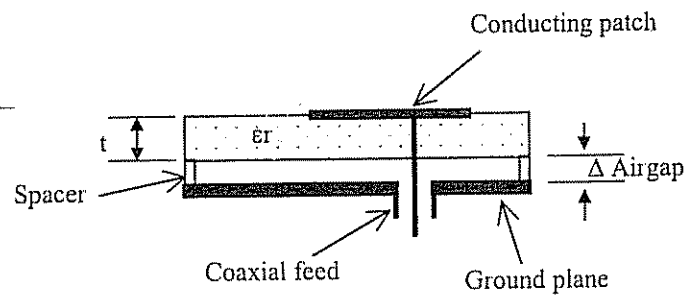
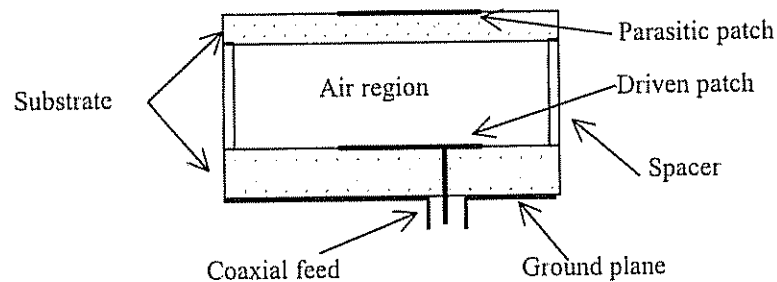

Figure 5.2 Microstrip antenna with airgap

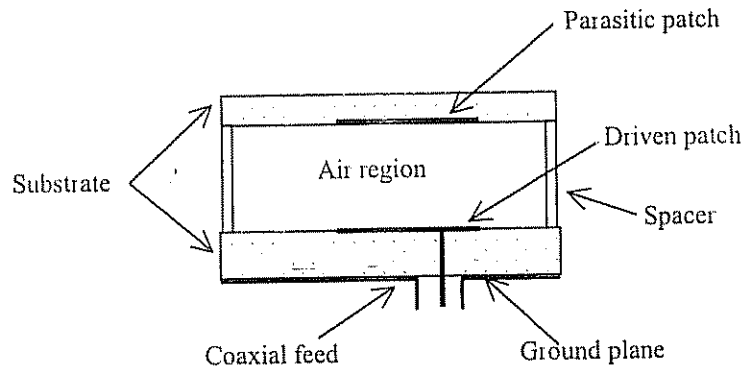Figure 5.3 Electromagnetically-coupled microstrip antenna

Figure 5.4 Inverted configuration of an electromagnetically coupled microstrip antenna

In figure 4.3, circular, annular-ring, rectangular and square patches etched on substrate about 0.01λ thick were reported to obtain bandwidth ranging from 9 % to 15 %. While in figure 4.4 the structure is referred to as the inverted configuration, the top patch is inverted so that the substrate is uppermost. The advantage of this kind of antenna is that it provides a protective dielectric cover for the conducting patch. Based on the lowest mode of the antenna studied, this configuration is capable of achieving 10 % bandwidth.

5.4 Broadband Microstrip Antennas Using Parasitic Elements Coupled To The Main Patch [73 - 77]

The method uses parasitic coplanar metallic strips coupled to the main patch as shown in figure 4.5. It first appear in 1978 [73]; however, the antenna was more like an array and subsequently, a novel broadband microstrip was introduced [74 - 77] using additional resonators that were gap coupled to the radiating edges of the main patch. Bandwidth up to 6.7 times that of a single rectangular patch antenna were reported. Different versions of these antennas have been studied, such as the triangular resonator [76], one parasitic patch [77] and a broadband gap-coupled microstrip antenna.
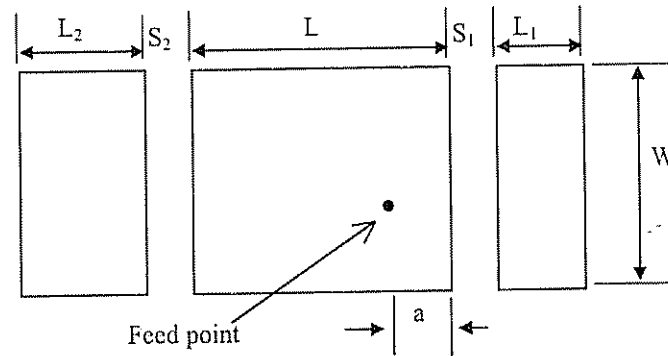
Figure 5.5 Coplanar parasitic tuned microstrip patch

5.5 Log-periodic And Quasi-log Periodic Techniques [78 - 80]

Using the concept of log-periodic antenna, the low and high frequency limits of the bandwidth are set by the largest and smallest dimensions of the structure respectively. Using this idea, Hall [78] and Pues et. al. [79] have proposed completely log-periodic and quasi log-periodic antennas respectively. The quasi-log-periodic antenna was achieved by arraying different narrow bandwidth radiators, each having its own frequency band of operation. The main advantages are the absence of an array effect in the E-plane and the fact that the antenna can be designed for specific degree of matching by the proper choice of spacing between the resonant frequencies, namely, the log-periodic expansion factor. The measured bandwidth for an VSWR ≤ 2.6 was 22 %, an improvement of approximately 10 times [79]. A nine-element completely log-periodic antenna published by Hall [78] reported 30 % bandwidth for an VSWR ≤ 2.2 and 70 % efficiency. Other studies [80] for a log-periodic array of narrow rectangular microstrip elements indicated that bandwidth at least as great as 50 % can be achieved.

5.6   Microstrip Patch Antennas With Tuning Stubs And Loads [81 - 83]

The frequency of operation of microstrip antennas can be selected or shifted without significantly varying the bandwidth by using tuning stubs [81]. Both resonant frequency and reflection coefficient of microstrip antennas are tuned using two tuning stubs in a coaxial fed patch. It was reported that the practical tuning range was limited by the length of the stubs as a long stub tends to degrade the matching condition. This was overcame by varying two tuning stubs [82], positioned on opposite edges of the patch, in line with the coaxial feed point, as shown in figure 5.6. The patch is tuned by systematic trimming off either of the stubs and due to the destructive nature of trimming techniques, the specific frequency of operation and the reflection coefficient can only be tuned from low to high frequency. Another application of tuning stubs is shown in figure 5.7 [83]. Here, an adjustable length short-circuited coaxial tuning stub was used. The spacing between the bands can be controlled by increasing the characteristic impedance of the loading stub, through increasing its length or by changing the inset of the load position.
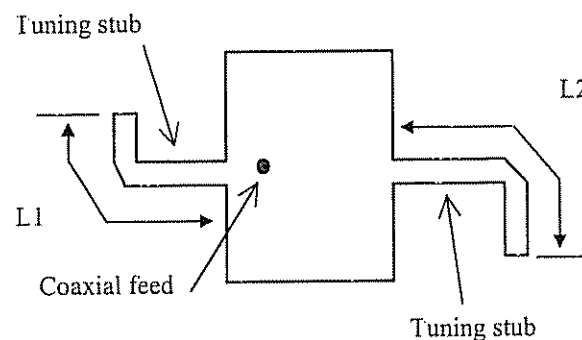

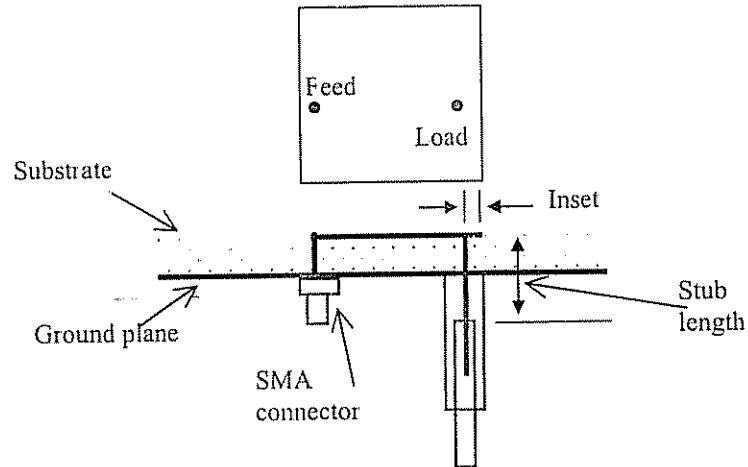Figure 5.6 Microstrip patch antenna with microstrip tuning stub

Figure 5.7 A reactively loaded microstrip antenna

5.7 Microstrip Antenna With Diodes (Frequency Agile Microstrip Antennas) [84 - 85]

By replacing the tuning stubs on the antenna as discussed in section 4.6 above with varactor or PIN diodes, the frequency of operation of microstrip antennas can be electronically selected or shifted without significantly varying the bandwidth. Because of this flexibility in tuning, these type of antennas are also known as frequency agile microstrip antennas. The geometrical structure of a varactor tuned microstrip antenna [84] is as shown in figure 5.8. It comprises of a circular disc antenna, the centre of the disc is shorted to the ground plane and the inner of the SMA connector is placed at a distance of one third of the radius away from the centre of the disc. The varactor diode is placed very close to the edge of the disc and coupled to the latter by using a lowloss chip capacitor. The $\frac{\lambda_m}{4}$ transmission line and a pad, used for biasing the varactor diode is also introduced. This technique produced two tunable modes which depended on the bias voltage applied to the varactor diode. Optically controlled PIN diodes were also used [85] to enhance the operating frequency range of the patch. The geometrical structure of this antenna is as shown in figure 5.9 where the parasitic element increased

45

the gain and performed a dual-frequency operation and did not disturb the radiation pattern.

5.8   Shorting Pin Technique [86]

Utilising a shorting pin is another interesting study that was carried out for frequency agile and polarisation diverse antenna [86]. By changing the number and location of the pin, the operating frequency can be tuned over a 1.5 to 1 range and the polarisation can be changed from horizontal to vertical, or right-hand to left-hand circular. Tuning ranges in excess of 50 percent are achieved by adding more posts. It was reported that the radiation patterns are not changed significantly by the shorting posts [86].
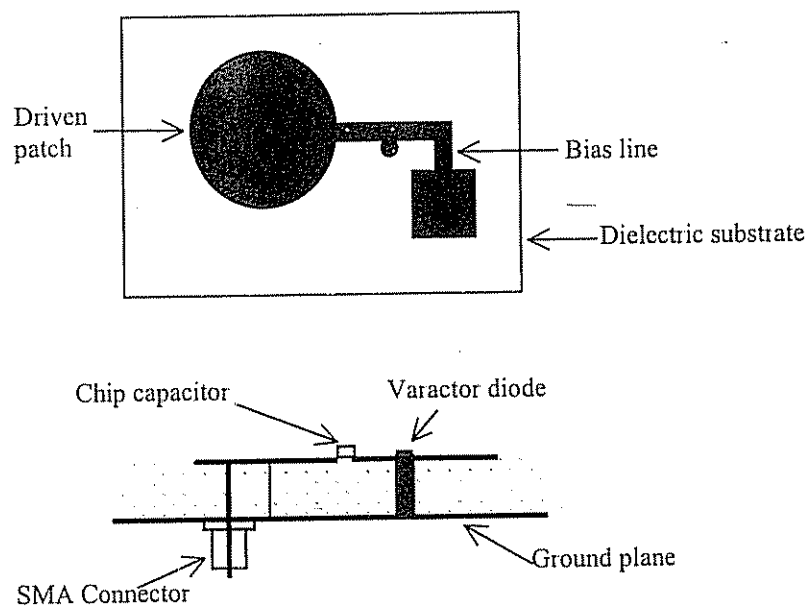

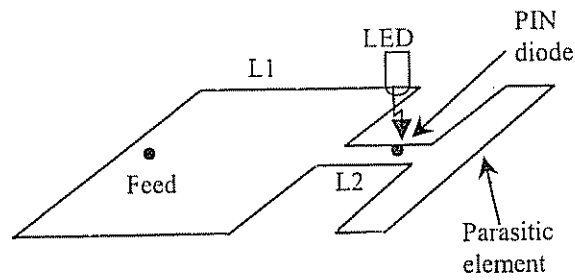Figure 5.8 Microstrip antenna with a varactor diode

Figure 5.9 A tunable antenna using an optically controlled PIN diode

5.9 Patches With Special Shape Or Techniques [87 - 89]

Simple antenna patches that were modified to form new shapes have been studied in the past and have been found to enhance the bandwidth. The following are several specially shaped patches to achieve the bandwidth enhancement. A slotted circular patch [87] as shown in figure 5.10 with a shunt conducting strip was reported to achieve 1.9 % bandwidth with VSWR of ≤ 2. The bow-tie antenna [88] shown in figure 5.11 is a planar antenna with inherent broadband impedance. This antenna has been used in superconducting tunnel junction and Schottky diode mixers in the frequency range of 94 to 466 GHz, and in linear imaging arrays, plasma diagnostic systems and radio astronomy. Research work has also been reported on the folded dipole radiator above a ground plane [89]. For the dipole shown in figure 5.12, the experimental data has shown a 5.5 % total bandwidth under a VSWR of 2.

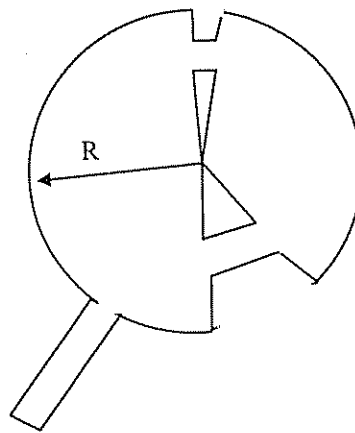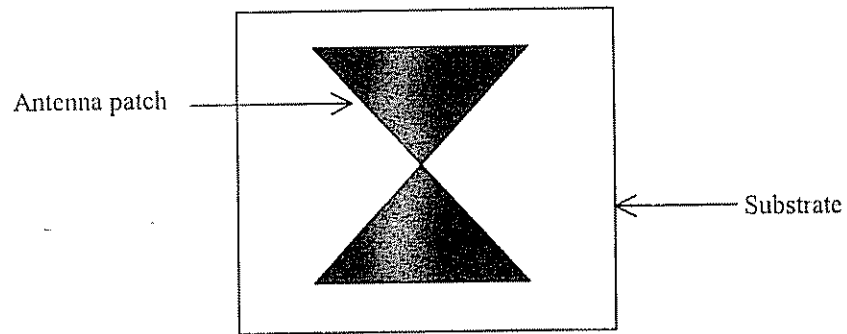Figure 5.10 A modified circular patch antenna
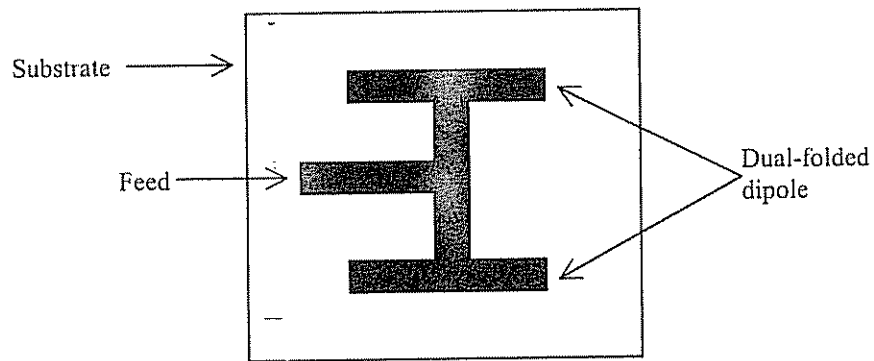
Figure 5.11 The bow-tie antenna

Figure 5.12 The dual-folded dipole

The improvement in bandwidth of the patch antennas can also be achieved by using stepped microstrip as shown in figure 5.13 or wedge shaped microstrip as shown in figure 5.14 . The bandwidths reported [90] for these structures were up to 25 %.
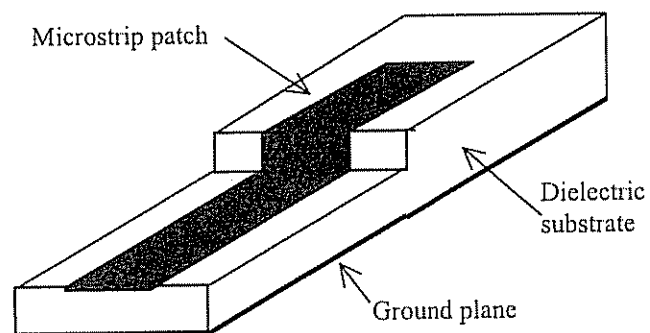
Figure 5.13 Stepped microstrip antenna

48
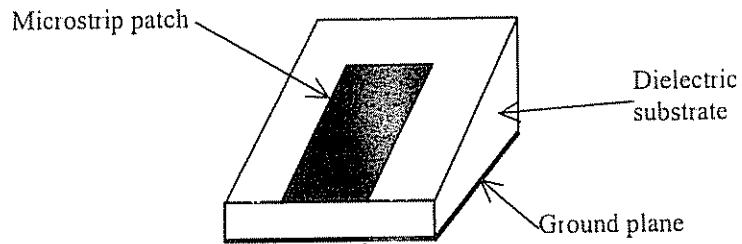
Figure 5. 14 Wedge-shaped microstrip antenna

Multi-layer microstrip antennas with line feeding [91] as shown in figure 5.15 (a) and (b) can also provide wide bandwidth. The wide bandwidth is achieved by employing the technique of a microstrip planar-array antenna which uses capacitive coupling to radiating elements or separate substrate overlaying the feed lines as shown. It was found that, further improvement in bandwidth could be obtained by using several layers of thinner substrate as shown in figure 5.15 (b).

Figure 5.15 (a) 2-Layer resonant antenna fed by open-circuit
microstrip line

Feed

Radiating patch

εr1

εr2

εr3

Ground plane

Figure 5.15 (b) 3-layer resonant antenna fed by open-circuit
microstrip line

5.10 Discussion

This chapter has presented a survey of several different antenna structures to achieve
dual- or wideband operation frequency in either a single element patch antenna or a
multi-element scheme. A closer study of the reviewed structures reveals that most of the
examples suffer from problems such as the difficulty to design or manufacture, and the
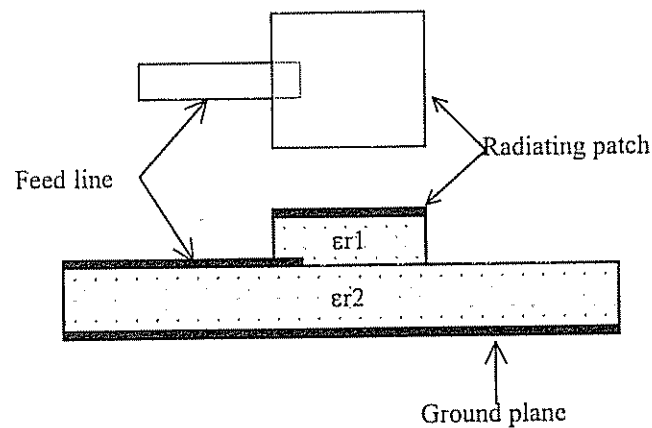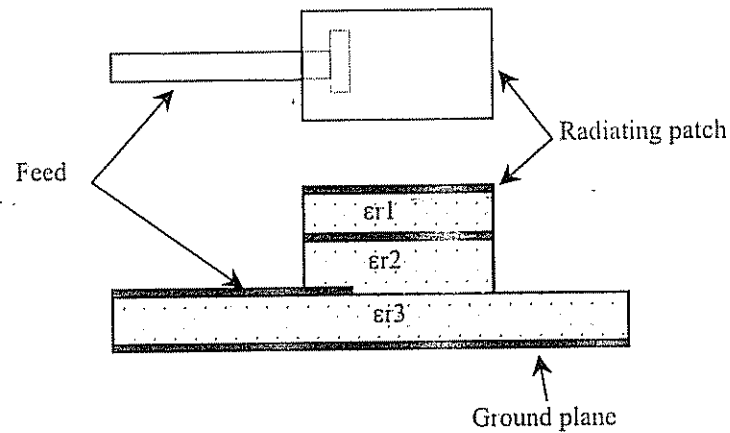increase in size or degradation in any of the other characteristics. Thus when choosing
or designing a wideband microstrip antenna for a particular application, one has to
balance between the needs for wideband operation and other characteristics such as size,
ease in design and fabrication and radiation patterns. By introducing slots in the patch,
the dual-frequency operation can be achieved in a single-element patch antenna. An
overall bandwidth enhancement up to 7.5% can be achieved with slotted patches and
although this improvement is much less than the 20% possible with multilayer
structures or 50% possible with log-periodic structures, no deterioration is observed or
reported on any of the other characteristics, such as size, height or radiation patterns
[58]. No one type of microstrip antenna will satisfy every design specification and in
this project novel design techniques to produce wideband antennas will be proposed and
as mentioned above suffer from similar problems.

50

CHAPTER VI

BANDWIDTH ENHANCEMENT THROUGH STACKED PARASITIC PATCH

6.1 Introduction

In chapter 5 the methods to enhance the bandwidth using stacked parasitic patch described in several published papers has been discussed briefly and on a closer examination of these papers revealed that none of them actually described the design procedures they were using to design the antenna in great detail and it was not possible to repeat the results for different frequency of operation. The feeding techniques described in some of the papers suggested that the authors were trying to match the feeding probe to the driven patch firstly and then adding the parasitic patch to the antenna to enhance the bandwidth. While this technique seems to achieve its objectives, it is not easily implemented as a general design technique. Two questions arise from studying those papers. Firstly, how the location of the feeding probe is selected? and secondly what is the function of the parasitic element? Without answering these two questions, the design of wideband antenna using stacked parasitic patch would need a lot of guess works. It was felt that a proper design technique that eliminates the guess works could be found from stacked parasitic patch. Experiment and calculation were carried out on several stacked antennas and have resulted in a new design technique being proposed and this will be described next.

6.2   Stacking Technique To Enhance The impedance Bandwidth

Experimental investigation into this technique revealed that a wide bandwidth antenna is achieved repeatedly when the following design steps are implemented.

1. The location of the feeding probe must be chosen at a point where the mismatching between probe and the driven patch is high such as at the corner of the driven patch.

2. The stacked parasitic patch is used as a tuning device to tune out the mismatching created by step 1 over a wider bandwidth. The height between it and the driven patch is use as the tuning variable.

Effectively, step 1 defined the location of the probe and can be found either experimentally or theoretically from a single patch antenna while step 2 defined the function of the parasitic patch. Since the location of a high mismatching for a single patch can be readily calculated using the existing method of analysis or measured experimentally, this has removed the guess works associated with the design of antenna using stacked parasitic patch as previously described.

6.3   Proposed Design Steps For Achieving Bandwidth Enhancement

With the inclusion of the two steps above, it is possible to propose a proper design step for using stacked parasitic patch to enhance the bandwidth of a probe fed single patch microstrip antenna from a few percent to at least 10%. These design steps are summarized in a flow chart as shown in figure 6.1 below.

```
┌─────────────────────────────────────┐
│                start                │
└─────────────────────────────────────┘
                   │
                   ▼
┌─────────────────────────────────────┐
│   Choose the shape of the driven patch │
└─────────────────────────────────────┘
                   │
                   ▼
┌─────────────────────────────────────┐
│   Design the driven patch to operate at │
│    the center frequency of operation │
└─────────────────────────────────────┘
                   │
                   ▼
┌─────────────────────────────────────┐
│   Locate the feeding probe using step A │
│           in section 6.1            │
└─────────────────────────────────────┘
                   │
                   ▼
┌─────────────────────────────────────┐
│   Tune the driven patch using step B in │
│            section 6.1              │
└─────────────────────────────────────┘
                   │
                   ▼
┌─────────────────────────────────────┐
│                stop                 │
└─────────────────────────────────────┘
```
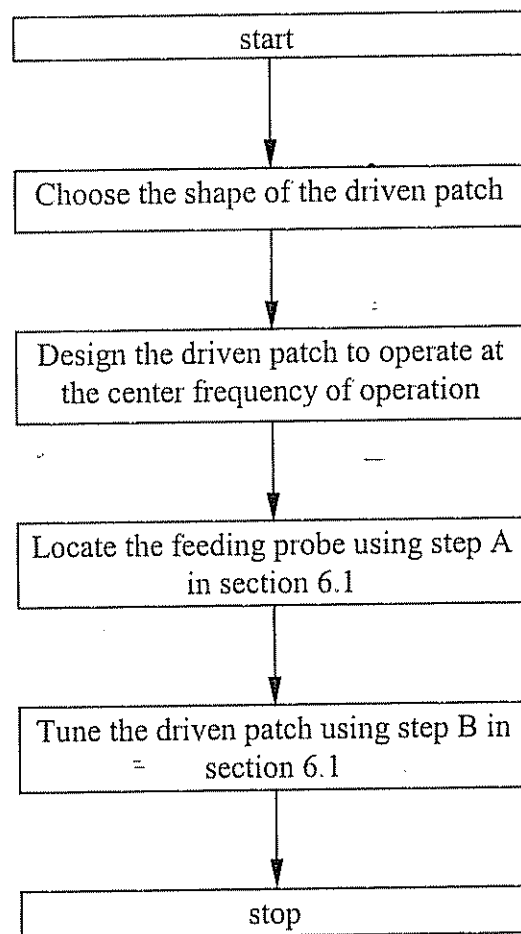
Figure 6.1 The proposed design steps.

These design steps have been used to design rectangular antennas at C-band frequencies. It was found that it has produced consistent results for all of them and will be discussed in the next sections.

53

6.4   Design of 4.7 to 6.2 GHz Wideband Microstrip Antenna

An antenna was designed to meet the following minimum technical specifications:

1. Center frequency = 5.5 GHz
2. Frequency bandwidth = 5.1 to 5.9 GHz
3. Half-power beam width = 60^0 (Elevation)

60^0 (Azimuth)

4. Nominal Input Impedance = 50 Ω
5. Polarization = Linear polarization.

These specifications were chosen since it could find applications in the industrial, scientific and medical frequency band as well as in the 3G wireless local area networks.

6.4.1 Antenna Configuration

The layout of the microstrip antenna is shown in figure 6.2b. Both driven and parasitic elements were fabricated using copper clad epoxy glass FR4 board having dielectric constant ε_r = 4.885 and thickness 1.57 mm. Epoxy glass FR4 was chosen as the substrate since it is readily available in the market and it is also cheaper compare to other substrates.

The driven patch was made of copper patch, situated on the surface of the driven substrate as shown in figure 6.2b and was designed to resonate initially at 4.5 GHz on its own without any suspended parasitic patch. This was found through mathematical calculation to give the desire frequency range needed later in the tuning process. The driven element was fabricated with dimensions as shown in figure 6.3a and 6.3b.
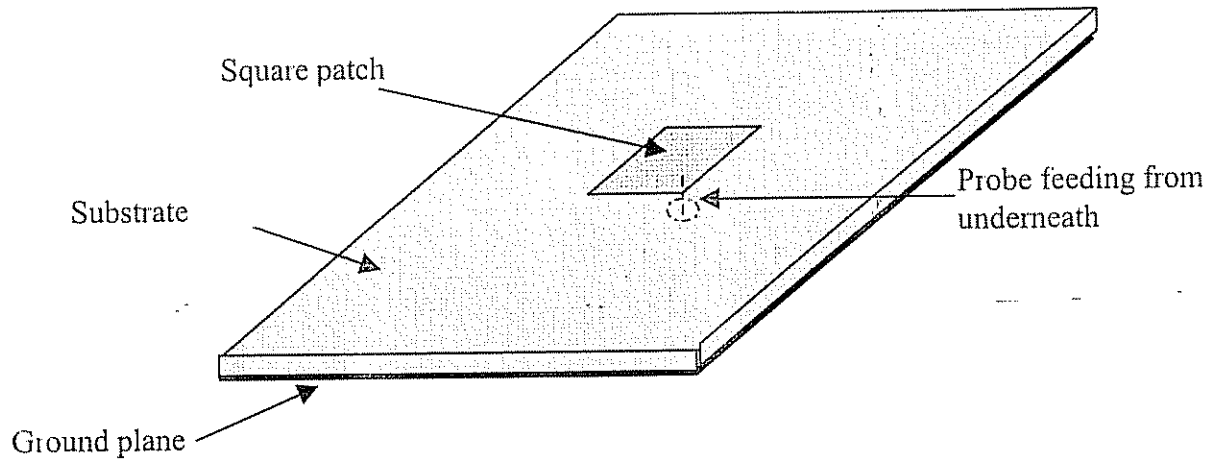
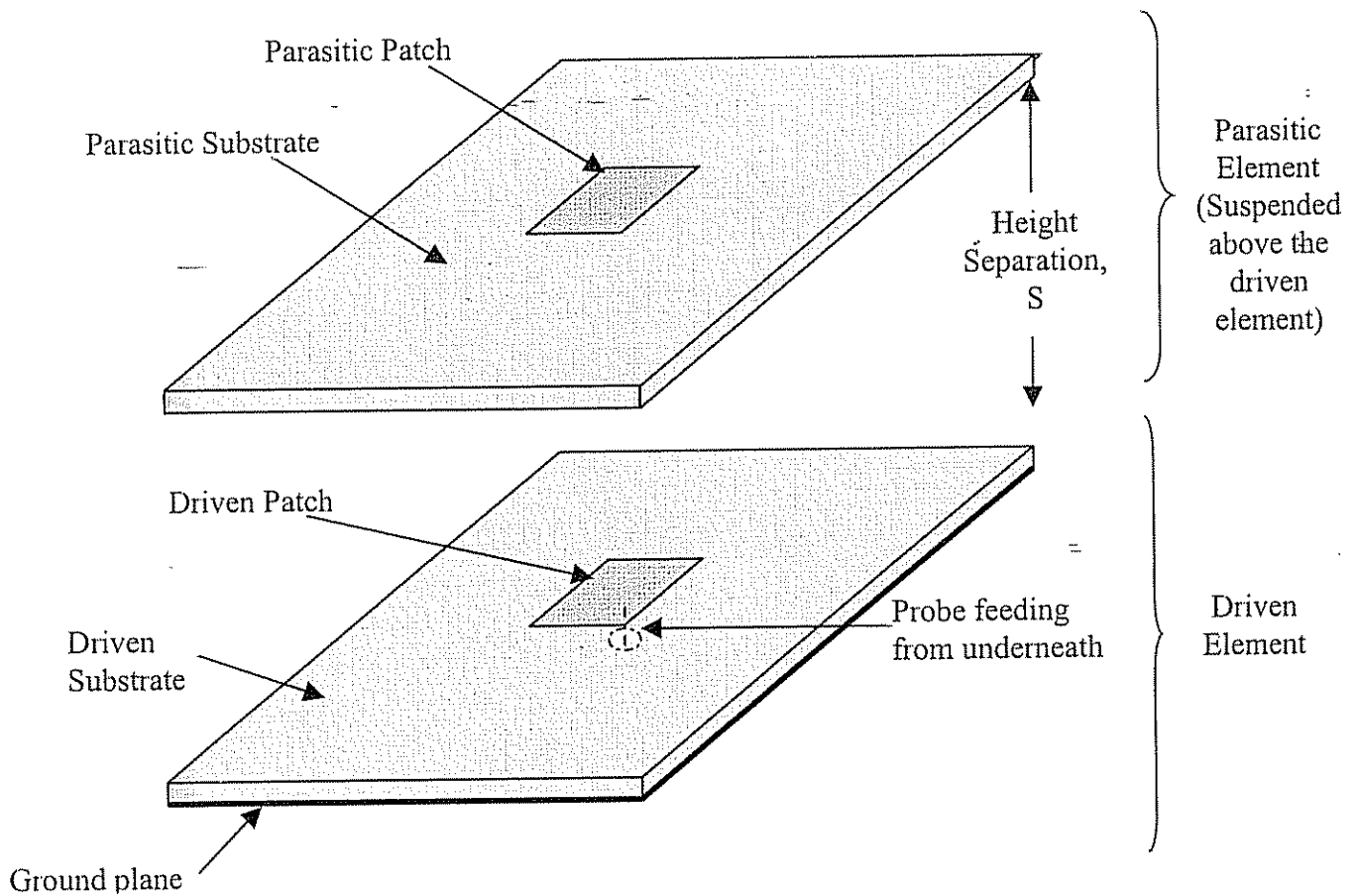figure 6.2a: A simple square microstrip patch antenna

Figure 6.2b: Square Microstrip Patch Antenna with Suspended Parasitic Element

Ground plane

Driven patch

Driven patch

45mm

14mm

122mm

Probe feeding.
(Modified SMA stub
contact panel socket)

ding probe location.
detail in figure 4)

strate.
uble sided copper
d epoxy glass FR4)

45mm

14mm

103mm

Side view

Figure 6.3a: Driven element

Parasitic patch

45mm

14mm

122mm

Parasitic patch

substrate
Double sided copper clad
poxy glass FR4 with
ottom copper removed)

45mm

14mm

103mm

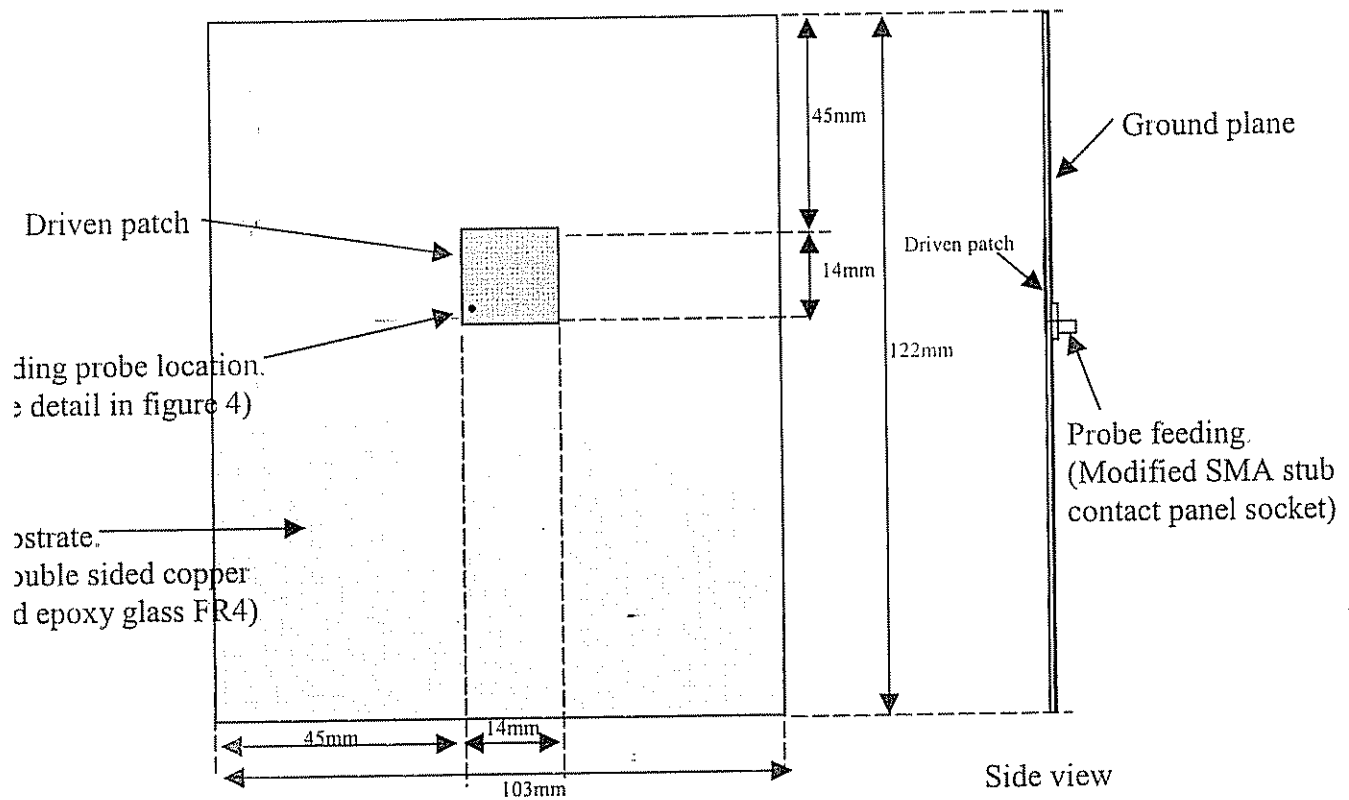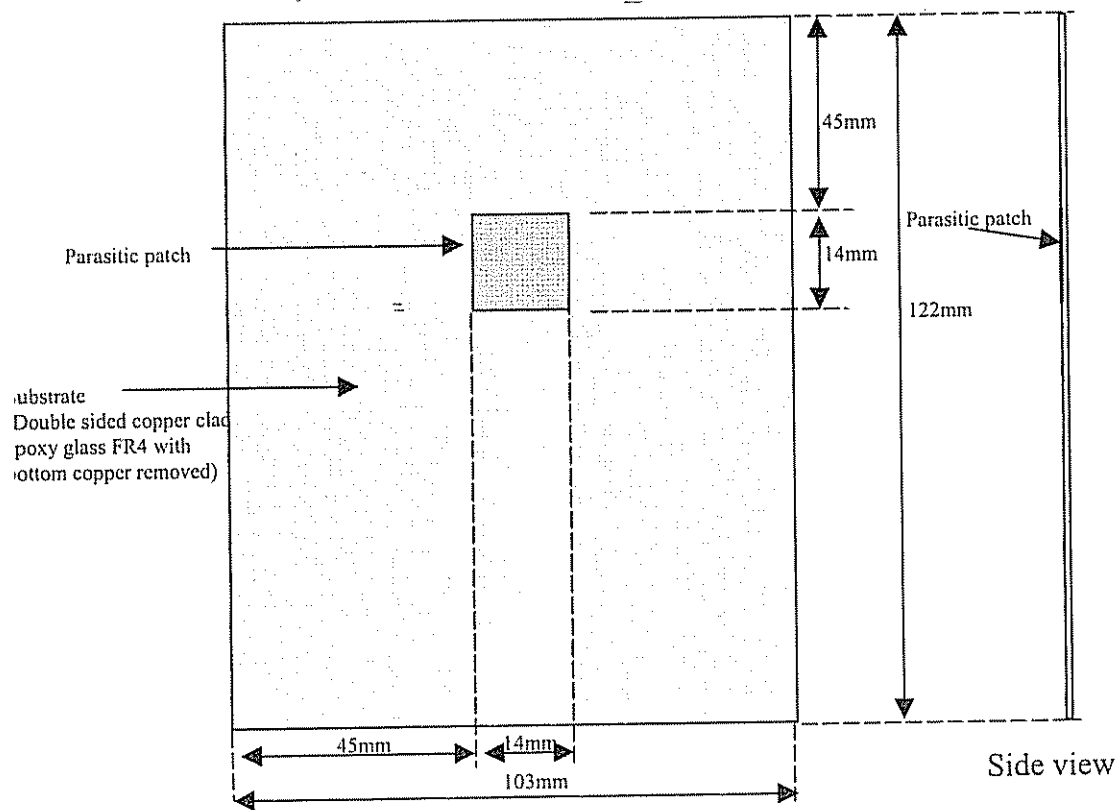Side view

Figure 6.3b. Parasitic element

56

For simplicity in design and fabrication, the parasitic element was fabricated using the same material and dimensions as driven element. Note that the only difference between parasitic element and driven element is that the later has a ground plane and a probe connection at the bottom while the former does not. There are two new design concepts that were introduced in the development of this antenna. The first concept is to locate and connect the feeding probe at one of the corner area of driven patch as shown in figure 6.4. It was found through mathematical calculation that the impedance mismatching between the probe and the driven patch is high in this region but relatively easily to alter using suspended parasitic element.
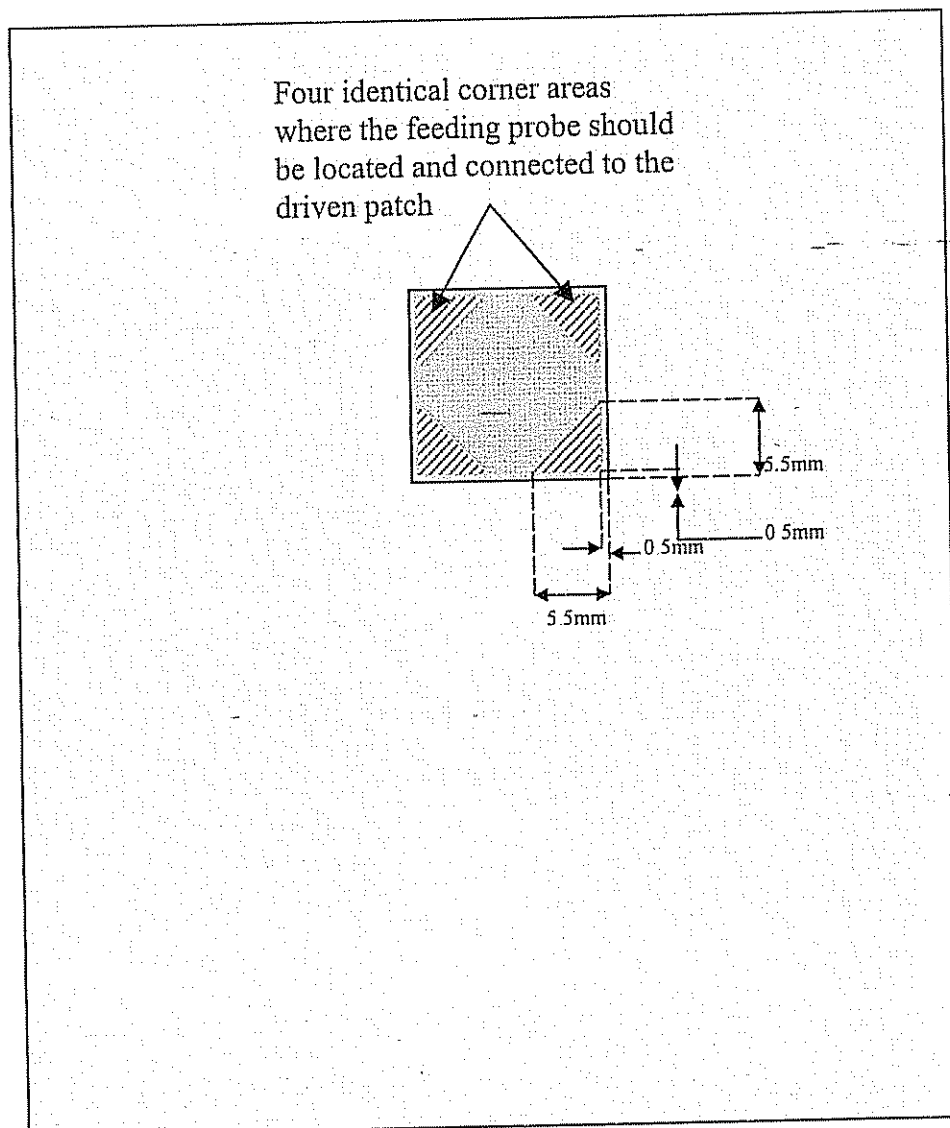

Figure 6.4: Four identical corner areas where the feeding probe should be located and connected

The second concept is to use the suspended parasitic element to tune out the impedance mismatching created by the first concept over a much wider bandwidth. The first design concept was developed through mathematical calculation of the S_{11} - parameter at various feeding location on the driven patch and observing its values varied during tuning process. The input impedance was calculated as follows:

$$f_{mn} = \frac{1}{2\sqrt{\mu_o \varepsilon_o \varepsilon_r}} \sqrt{\left(\frac{m}{a}\right)^2 + \left(\frac{n}{b}\right)^2} \qquad 6.1$$

where

f_{mn} = resonant frequency for mn mode

μ_o = free space permeability

ε_o = free space permittivity

ε_r = dielectric constant of the medium between the patch and the ground plane

m,n = positive integers

a = ideal length of the rectangular patch

b = ideal width of the rectangular patch

Let f_1, f_2 and f_c be the frequencies of the TM_{10}, TM_{01} modes and centre frequency respectively. For the design centre frequency of 4.5 GHz and square patch f_{10} and f_{01} were chosen to be equal to f_c. The ideal dimensions for the driven patch are given by

$$a = \frac{1}{2\sqrt{\mu_o \varepsilon_o \varepsilon_r} \cdot f_{01}} \qquad 6.2$$

$$b = \frac{1}{2\sqrt{\mu_o \varepsilon_o \varepsilon_r} \cdot f_{10}} \qquad 6.3$$

and the actual dimensions are given by

$$L = b - \Delta L \qquad 6.4$$
$$W = a - \Delta W \qquad 6.5$$

Where L and W are the length and width of the driven patch respectively; ΔL and ΔW are the corresponding corrections. The correction terms are found using the formula given by

$$\frac{\Delta L}{h} = 0.412 \left[\frac{\varepsilon_{rel} + 0.3}{\varepsilon_{rel} - 0.258} \right] \left[\frac{\frac{W}{h} + 0.262}{\frac{W}{h} + 0.813} \right] \times 2 \qquad 6.6$$

where

$$\varepsilon_{rel} = \frac{(\varepsilon_r + 1)}{2} + \frac{(\varepsilon_r - 1)}{2} \left[1 + \frac{10h}{W} \right]^{-0.555} \qquad 6.7$$

Since both TM_{10} and TM_{01} modes were used, it was found experimentally that better results can be achieved if W was also corrected using the same formula as follows

$$\frac{\Delta W}{h} = 0.412 \left[\frac{\varepsilon_{re2} + 0.3}{\varepsilon_{re2} - 0.258} \right] \left[\frac{\frac{L}{h} + 0.264}{\frac{L}{h} + 0.8} \right] \times 2 \qquad 6.8$$

where

$$\varepsilon_{re2} = \frac{(\varepsilon_r + 1)}{2} + \frac{(\varepsilon_r - 1)}{2} \left[1 + \frac{10h}{L} \right]^{-0.555} \qquad 6.9$$

The driven and parasitic patches were chosen to have the same dimensions and these were calculated by simultaneously solving equations 6.4 – 6.9 together with the calculated f_{10} and f_{01} values. For this case it was found that W = 14mm and L = 14mm. To locate the feeding probe, it was necessary to analyse the input impedance given by :

$$Zin = \sum_{m=0}^{\infty} \sum_{n=0}^{\infty} (\psi_m \psi_n)^2 \frac{\cos^2 \left(\frac{m\pi x_p}{a} \right) \cos^2 \left(\frac{n\pi y_p}{b} \right)}{j\omega C + \left(\frac{1}{j\omega L_{mn}} \right) + g_{mn}} \qquad 6.10$$

where

$$\psi_p = \begin{cases} 1, & p = 0 \\ \sqrt{2}, & p \neq 0 \end{cases}$$

x_p, y_p = The x and y coordinate of the probe respectively

$$C = \frac{\varepsilon_r \varepsilon_0 S_e}{h}$$

$$L_{mn} = \frac{1}{\omega_{mn}^2 C}$$

$$S_e = \text{effective patch area} = a*b$$

$$g_{mn} = g_c^{mn} + g_d^{mn} + g_r^{mn}$$

$$g_c^{mn} = \frac{2R_s}{h\mu_o}\left(\frac{\omega_{mn}}{\omega}\right)^2 C$$

$$g_r^{mn} = \frac{2S_e}{h^2}P_{ro}^{mn}$$

$$P_{ro}^{mn} = \frac{1}{2}\text{Re}\left\{\iint\left(\bar{E}_o^{mn*} \times \bar{H}_o^{mn}\right)\cdot\hat{R}\sin\theta d\theta d\phi\right\}$$

$$\bar{E}_o^{mn} = \eta_o\bar{H}_o^{mn}\times\hat{R} \qquad \left(0\le\theta\le\frac{\pi}{2}\right)$$

$$\bar{H}_o^{mn} = \frac{-j\omega\varepsilon_o}{4\pi}h\left[2\cos\left(\frac{k_o h}{2}\cos\theta\right)\right]\cdot\oint_{patch}\left(\hat{n}\times\hat{z}\right)\phi_{mn}(r)\exp(jk_o\bar{r}\cdot\hat{R})dl$$

$\bar{E}$ and $\bar{H}$ are the electric and magnetic field vectors in the cavity region respectively. $\hat{R}$ is the unit vector in the direction of R axis in polar coordinates and Re{} represent the real part in the braces. $\bar{r}$ is the vector from the coordinate origin to any point on the periphery of the patch and $\phi_{m,n}(r)$ is the value of the eigenfunction at the end of vector $\bar{r}$ is given by

$$\phi_{mn}(x,y) = \frac{\Psi_m\Psi_n}{\sqrt{S_e}}\cos\left(\frac{m\pi x}{a}\right)\cos\left(\frac{n\pi y}{b}\right) \qquad\qquad 6.11$$

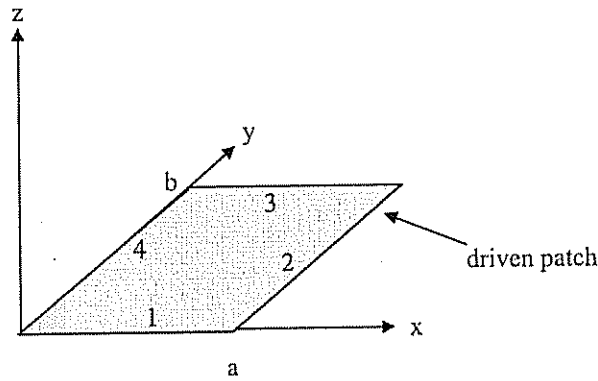The calculation of P_{ro}^{mn} (the radiated power) is give as follows;

Figure 6.5 Rectangular driven patch

60

For a rectangular driven patch as shown in figure 6.5, the radiated power is given by

$$P_{ro}^{mn} = \frac{1}{2} \operatorname{Re}\left\{ \iint \left(\bar{E}_o^{mn*} \times \bar{H}_o^{mn} \right) \cdot \hat{R} \sin\theta d\theta d\phi \right\} \qquad 6.12$$

$$\bar{E}_o^{mn} = \eta_o \bar{H}_o^{mn} \times \hat{R} \qquad \left(0 \le \theta \le \frac{\pi}{2} \right) \qquad 6.13$$

$$\bar{H}_o^{mn} = \frac{-j\omega\varepsilon_o}{4\pi} h \left[2\cos\left(\frac{k_o h}{2} \cos\theta \right) \right] \oint_{patch} (\hat{n} \times \hat{z}) \varphi_{mn}(r) \exp(jk_o \bar{r} \cdot \hat{R}) dl \qquad 6.14$$

$$\varphi_{mn}(x,y) = \frac{\Psi_m \Psi_n}{\sqrt{S_e}} \cos\left(\frac{m\pi x}{a} \right) \cos\left(\frac{n\pi y}{b} \right) \qquad 6.15$$

Let $\zeta = \dfrac{-j\omega\varepsilon_o}{4\pi} h \left[2\cos\left(\dfrac{k_o h}{2} \cos\theta \right) \right]$, then equation 6.14 can be rewritten as,

$$\bar{H}_o^{m,n} = \zeta \oint_{patch} (\hat{n} \times \hat{z}) \frac{\Psi_m \Psi_n}{\sqrt{S_e}} \cos\left(\frac{m\pi x}{a} \right) \cos\left(\frac{n\pi y}{b} \right) \exp(jk_o \bar{r} \cdot \hat{R}) dl \qquad 6.16$$

Substituting $\bar{r} \cdot \hat{R} = (x\cos\phi + y\sin\phi)\sin\theta$ into equation 6.16 gives,

$$\bar{H}_o^{mn} = \zeta \oint_{patch} (\hat{n} \times \hat{z}) \frac{\Psi_m \Psi_n}{\sqrt{S_e}} \cos\left(\frac{m\pi x}{a} \right) \cos\left(\frac{n\pi y}{b} \right) \exp(jk_o(x\cos\phi + y\sin\phi)\sin\theta) dl \qquad 6.17$$

Integrating over the boundaries gives,

Boundary (1): $\qquad \bar{H}_{o1}^{mn} = -\hat{x}\zeta \int_0^a \varphi_{mn}(x,0)\exp(jk_o(x\cos\phi)\sin\theta)dx \qquad$ 6.18

Boundary (2): $\qquad \bar{H}_{o2}^{mn} = -\hat{y}\zeta \int_0^b \varphi_{mn}(a,y)\exp(jk_o(a\cos\phi + y\sin\phi)\sin\theta)dy \qquad$ 6.19

Boundary (3): $\qquad \bar{H}_{o3}^{mn} = -\hat{x}\zeta \int_0^a \varphi_{mn}(x,b)\exp(jk_o(x\cos\phi + b\sin\phi)\sin\theta)dx \qquad$ 6.20

Boundary (4): $\qquad \bar{H}_{o4}^{mn} = -\hat{y}\zeta \int_0^b \varphi_{mn}(0,y)\exp(jk_o(y\sin\phi)\sin\theta)dy \qquad$ 6.21

Combining equations 6.18 and 6.20 to obtain the x-component of $\bar{H}_o^{m,n}$ field, gives

$$H_x^{mn} = -\zeta \int_0^a \left[\varphi_{mn}(x,0)\exp(jk_o x\cos\phi\sin\theta) + \varphi_{mn}(x,b)\exp\left(jk_o(x\cos\phi + b\sin\phi)\sin\theta\right)\right]dx \qquad 6.22$$

From equation 6.15, gives

$$\varphi_{mn}(x,0) = \frac{\Psi_m\Psi_n}{\sqrt{Se}}\cos\left(\frac{m\pi x}{a}\right) \qquad\qquad 6.23$$

$$\varphi_{mn}(x,b) = \frac{\Psi_m\Psi_n}{\sqrt{Se}}\cos\left(\frac{m\pi x}{a}\right)(-1)^n$$

$$= \varphi_{mn}(x,0)(-1)^n \qquad\qquad 6.24$$

Substitute equations 6.23 and 6.24 into equation 6.22 gives,

$$H_x^{mn} = -\zeta \int_0^a \left[\varphi_{mn}(x,0)\exp(jk_o x\cos\phi\sin\theta)\left(1 + (-1)^n \exp(jk_o b\sin\phi\sin\theta)\right)\right]dx \qquad 6.25$$

There are 5 conditions in calculating equation 6.25 as follows,

Condition 1:   if $\dfrac{m\pi}{k_o a} \neq \cos\phi\sin\theta \neq 0$ then

$$H_x^{mn} = -\zeta AD(BC + E) \qquad\qquad 6.26$$

where $\qquad A = 1 + (-1)^n \exp(jk_o b\sin\phi\sin\theta)$

$$B = -\sqrt{a}\,\exp(jk_o a\cos\phi\sin\theta)$$

$$C = jk_o a\cos\phi\sin\theta(-1)^m$$

$$D = \frac{\Psi_m\Psi_n}{\left((k_o a\cos\phi\sin\theta)^2 - (m\pi)^2\right)\sqrt{b}}$$

$$E = j(a)^{1/2}k_o\cos\phi\sin\theta$$

Condition 2:   if $\dfrac{m\pi}{k_o a} = \cos\phi\sin\theta \neq 0$ then

$$H_x^{mn} = -\zeta \int_0^a \left[\varphi_{mn}(x,0)\exp\left(jk_o x\left(\frac{m\pi}{k_o a}\right)\right)\left(1 + (-1)^n \exp(jk_o b\sin\phi\sin\theta)\right)\right]dx$$

62

$$= -\zeta AG\left[F + j\frac{\sqrt{a}}{2}\right] \qquad\qquad 6.27$$

where $\qquad F = \frac{1}{2}\sqrt{a}\left(m\pi - j\right)$

$$G = \frac{\Psi_m \Psi_n}{m\pi\sqrt{b}}$$

Condition 3:   if $\dfrac{m\pi}{k_o a} = 0,\ \cos\phi\sin\theta \neq 0$ then

$$H_x^{mn} = -\zeta\int_0^a\left[\frac{\Psi_m\Psi_n}{\sqrt{Se}}\exp\left(jk_o x\cos\phi\sin\theta\right)\left(1 + (-1)^n\exp\left(jk_o b\sin\phi\sin\theta\right)\right)\right]dx$$

$$= -\zeta AH(1 - I) \qquad\qquad 6.28$$

where $\qquad H = \dfrac{j\Psi_m\Psi_n}{k_o\cos\phi\sin\theta\sqrt{Se}}$

$$I = \exp(jk_o a\cos\phi\sin\theta)$$

Condition 4:   if $\dfrac{m\pi}{k_o a} \neq 0,\ \cos\phi\sin\theta = 0$ then

$$H_x^{mn} = -\zeta\int_0^a\left[\frac{\Psi_m\Psi_n}{\sqrt{Se}}\cos\left(\frac{m\pi x}{a}\right)\left(1 + (-1)^n\exp\left(jk_o b\sin\phi\sin\theta\right)\right)\right]dx$$

$$= -\zeta A\frac{\sin(m\pi)}{m\pi}\sqrt{a}\,\frac{\Psi_m\Psi_n}{\sqrt{b}}$$

$$= 0 \qquad \text{since } \sin(m\pi) = 0\ \forall\ m = \text{ positive integer} \qquad 6.29$$

Condition 5:   if $\dfrac{m\pi}{k_o a} = 0 = \cos\phi\sin\theta = 0$ then

$$H_x^{mn} = -\zeta\int_0^a\left[\frac{\Psi_m\Psi_n}{\sqrt{Se}}\left(1 + (-1)^n\exp\left(jk_o b\sin\phi\sin\theta\right)\right)\right]dx$$

$$= -\zeta A\left(\frac{\Psi_m \Psi_n}{\sqrt{Se}}\right)a \qquad\qquad 6.30$$

Combining equations 6.19 and 6.21 to obtain the y-component of $\bar{H}_o^{mn}$ field, gives

$$H_y^{mn} = -\zeta \int_0^b \varphi(0,y)\exp(jk_o\sin\phi\sin\theta)(1+(-1)^m jk_o a\cos\phi\sin\theta)dy \qquad 6.31$$

Similar to the x-component of $\bar{H}_o^{mn}$ field, there are 5 conditions to solve equation 6.31 as follows.

Condition 1:   if $\dfrac{n\pi}{bk_o} \neq \sin\phi\sin\theta \neq 0$ then

$$H_y^{mn} = -\zeta JM(KL + N) \qquad\qquad 6.32$$

where $\qquad J = 1 + (-1)^m \exp(jk_o a\cos\phi\sin\theta)$

$$K = -\sqrt{b}\exp(jk_o b\sin\phi\sin\theta$$

$$L = jk_o b\sin\phi\sin\theta(-1)^n$$

$$M = \frac{\Psi_m \Psi_n}{\left(\left(k_o b\sin\phi\sin\theta\right)^2 - \left(n\pi\right)^2\right)\sqrt{a}}$$

$$N = jb^{3/2}k_o\sin\phi\sin\theta$$

Condition 2:   if $\dfrac{n\pi}{bk_o} = \sin\phi\sin\theta \neq 0$ then

$$H_y^{mn} = -\zeta \int_0^b \frac{\Psi_m \Psi_n}{\sqrt{Se}}\cos\left(\frac{n\pi y}{b}\right)\exp\left(jk_o\left(\frac{n\pi}{k_o b}\right)\right)(1+(-1)^m jk_o a\cos\phi\sin\theta)dy$$

$$= -\zeta JP\left(O + \frac{j\sqrt{b}}{2}\right) \qquad\qquad 6.33$$

where $\qquad O = \dfrac{\sqrt{b}}{2}(n\pi - j)$

64

$$P = \frac{\Psi_m \Psi_n}{n\left(\pi\sqrt{a}\right)}$$

Condition 3:   if $\dfrac{n\pi}{k_o b} = 0$, $\sin\phi\sin\theta \neq 0$ then

$$H_y^{mn} = -\zeta \int_0^b \left[\frac{\Psi_m \Psi_n}{\sqrt{Se}} \exp\left(jk_o y \sin\phi\sin\theta\right)\left(1 + (-1)^m \exp\left(jk_o a \cos\phi\sin\theta\right)\right)\right] dy$$

$$= -\zeta JQ(1-R) \qquad\qquad 6.34$$

where $\qquad Q = \dfrac{j\Psi_m \Psi_n}{k_o \sin\phi\sin\theta \sqrt{Se}}$

$$R = \exp\left(jk_o b \sin\phi\sin\theta\right)$$

Condition 4:   if $\dfrac{n\pi}{k_o b} \neq 0$, $\sin\phi\sin\theta = 0$ then

$$H_y^{mn} = -\zeta \int_0^b \left[\frac{\Psi_m \Psi_n}{\sqrt{Se}} \cos\left(\frac{n\pi y}{b}\right)\left(1 + (-1)^m \exp\left(jk_o a \cos\phi\sin\theta\right)\right)\right] dy$$

$$= -\zeta J \frac{\sin(n\pi)}{n\pi} \sqrt{b} \frac{\Psi_m \Psi_n}{\sqrt{a}}$$

$$= 0 \qquad \text{since } \sin(n\pi) = 0 \; \forall \; n = \text{ positive integer} \qquad 6.35$$

Condition 5:   if $\dfrac{n\pi}{k_o b} = 0 = \sin\phi\sin\theta = 0$ then

$$H_y^{mn} = -\zeta \int_0^b \left[\frac{\Psi_m \Psi_n}{\sqrt{Se}} \left(1 + (-1)^m \exp\left(jk_o a \cos\phi\sin\theta\right)\right)\right] dy$$

$$= -\zeta J \left(\frac{\Psi_m \Psi_n}{\sqrt{Se}}\right) b \qquad\qquad 6.36$$

The total magnetic field $\vec{H}_o^{mn}$ is given by

$$\vec{H}_o^{mn} = \hat{x} H_x^{mn} + \hat{y} H_y^{mn} \qquad\qquad 6.37$$

Once the equations for $\vec{H}_o^{mn}$ has been established, $\vec{E}_o^{mn*}$ is given by

$$\bar{E}_o^{mn*} = \eta_o\left(\bar{H}_o^{mn*} \times \hat{R}\right)$$

$$\Rightarrow \bar{E}_o^{mn*} = \eta_o\left[\hat{x}\left(H_y^{mn*}R_z\right) - \hat{y}\left(H_x^{mn*}R_z\right) + \hat{z}\left(H_x^{mn*}R_y - H_y^{mn*}R_x\right)\right] \qquad 6.38$$

$$\Rightarrow \bar{E}_o^{mn*} \times \bar{H}_o^{mn} = \eta_o\begin{bmatrix}\hat{x}\left(H_y^{mn}H_y^{mn*}R_x - H_y^{mn}H_x^{mn*}R_y\right)\\[4pt] +\hat{y}\left(H_x^{mn}H_x^{mn*}R_{y'} - H_x^{mn}H_y^{mn*}R_x\right)\\[4pt] +\hat{z}\left(H_y^{mn}H_y^{mn*}R_z + H_x^{mn}H_x^{mn*}R_z\right)\end{bmatrix} \qquad 6.39$$

$$\Rightarrow \left(\bar{E}_o^{mn*} \times \bar{H}_o^{mn}\right)\cdot\hat{R} = \eta_o\left(\begin{array}{l}R_x^2\left|H_y^{mn}\right|^2 - R_xR_y\left(H_y^{mn}H_x^{mn*} + H_x^{mn}H_y^{mn*}\right)\\[4pt] +R_y^2\left|H_x^{mn}\right|^2 + R_z^2\left(\left|H_x^{mn}\right|^2 + \left|H_y^{mn}\right|^2\right)\end{array}\right) \qquad 6.40$$

Substituting for R_x, R_y and R_z gives

$$\Rightarrow \left(\bar{E}_o^{mn*} \times \bar{H}_o^{mn}\right)\cdot\hat{R} = \eta_o\left(\begin{array}{l}\left(\sin^2\theta\sin^2\phi + \cos^2\theta\right)\left|H_x^{mn}\right|^2 + \left(\sin^2\theta\cos^2\phi + \cos^2\theta\right)\left|H_{y^-}^{mn}\right|^2\\[4pt] -\sin^2\theta\sin\phi\cos\phi\left(H_x^{mn}H_y^{mn*} + H_y^{mn}H_x^{mn*}\right)\end{array}\right) \qquad 6.41$$

Substituting equation 6.41 into equation 6.12 gives

$$P_{ro}^{mn} = \frac{1}{2}\mathrm{Re}\left\{\iint \eta_o\left(\begin{array}{l}\left(\sin^2\theta\sin^2\phi + \cos^2\theta\right)\left|H_x^{mn}\right|^2 + \left(\sin^2\theta\cos^2\phi + \cos^2\theta\right)\left|H_y^{mn}\right|^2\\[4pt] -\sin^2\theta\sin\phi\cos\phi\left(H_x^{mn}H_y^{mn*} + H_y^{mn}H_x^{mn*}\right)\end{array}\right)\sin\theta\, d\theta\, d\phi\right\} \qquad 6.42$$

Equation 6.42 is calculated numerically to obtain the radiated power due to TM_{mn} mode from the rectangular microstrip patch antenna. Using equation 6.10 to calculate the return loss, figure 6.5 shows those values at various probe locations on the surface of the driven patch when excited at TM_{10} and TM_{01} mode frequencies. It shows that the probe location in the middle of the driven patch gives maximum mismatching for both TM_{01} and TM_{10} modes. However, experimental and simulation works reveal that at this location the mismatching is a hard mismatching that cannot readily modified using simple suspended parasitic tuning element. The next location would be at the corners of the patch where they also give high mismatching. With this location it was found that the mismatching could readily be matched using simple suspended parasitic tuning element.
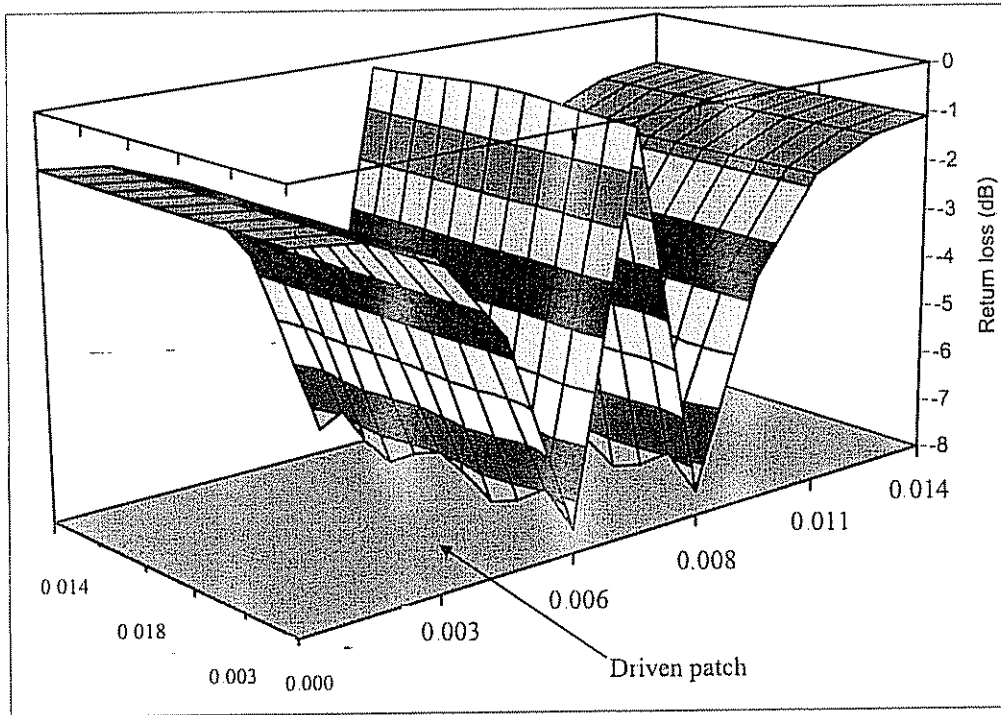
Return loss values excited at TM10 mode frequency
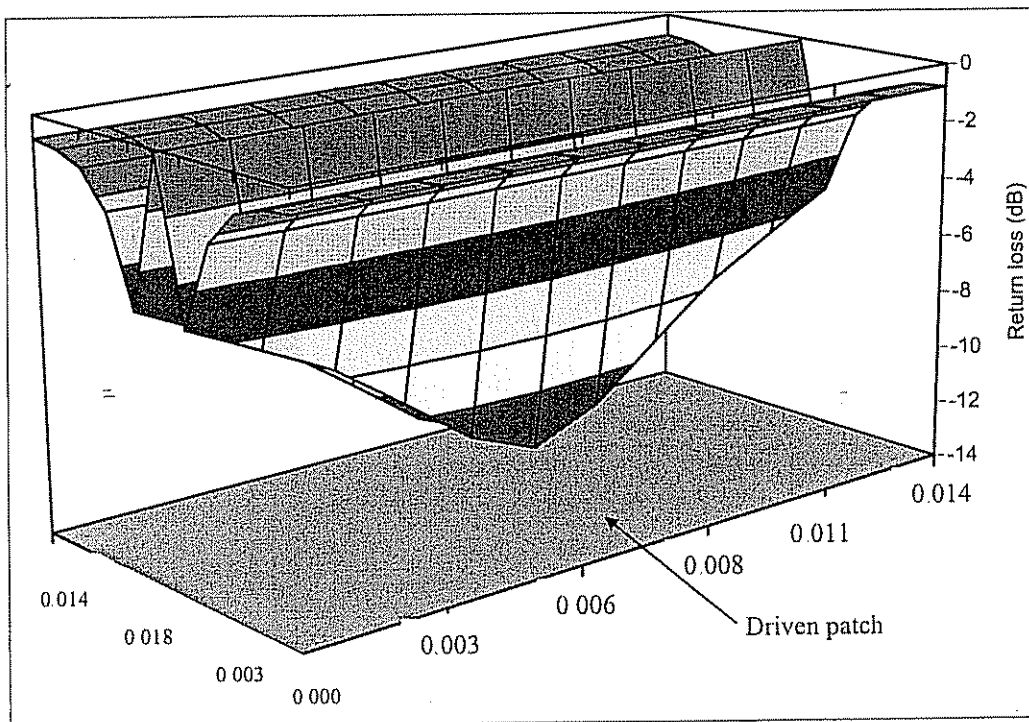
Return loss values excited at TM01 mode frequency

Figure 6.5   The values of return loss at various points on the driven patch
when excited at TM10 and TM01 mode frequencies

67

The parasitic patch was chosen to be the same as the driven patch and as the height separation was gradually increased, experimental observations showed that at a particular height the maximum impedance matching condition at the two distinct frequencies corresponding nearly to the TM_{10} and TM_{01} modes were obtained. As shown in figure 6.6 beyond this point, as the height separation was increased further, the antenna started to match the impedance for frequencies in between the two modes at the expense of the matching conditions of the latter.
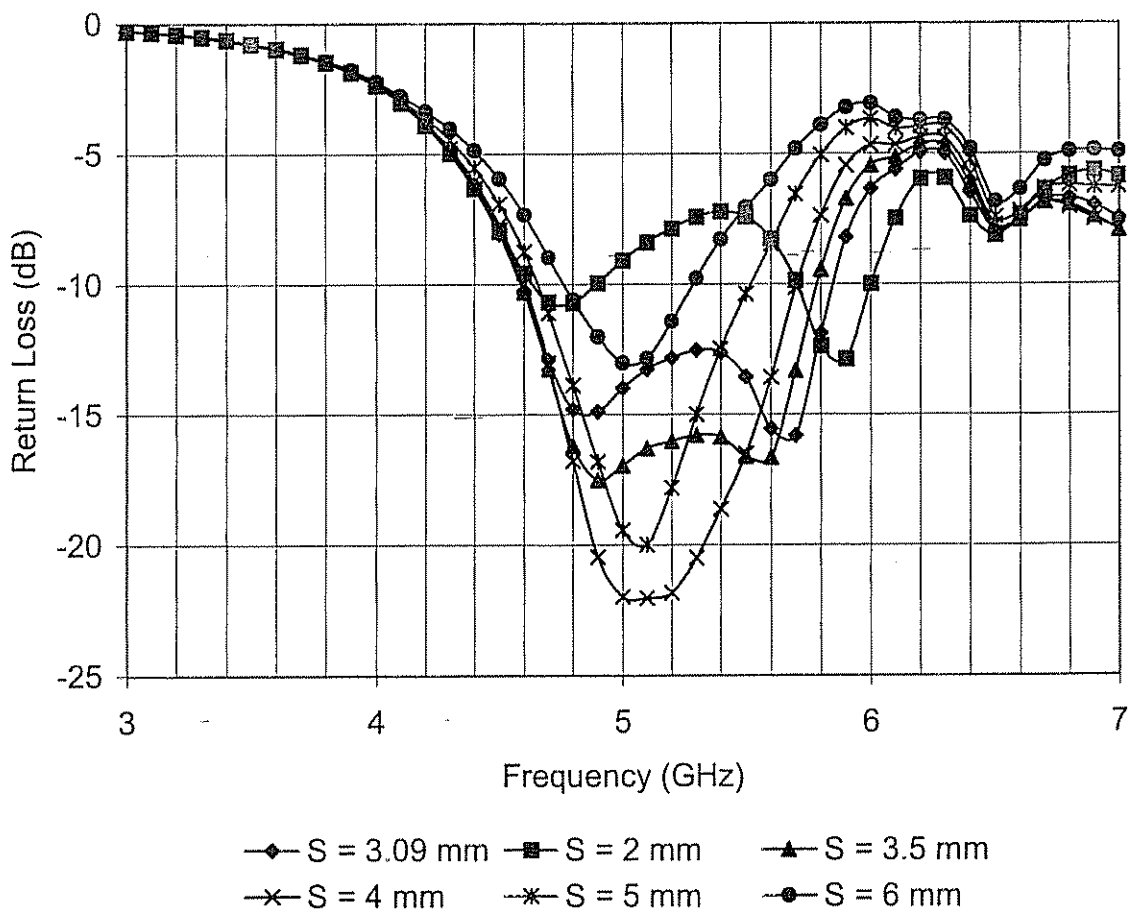

Figure 6.6 The effect of varying the height separation between elements.

At optimum impedance bandwidth, it was measured to be 1.401 GHz at the separation height, S = 3.09 mm. Figure 6.7 illustrates the dependence of return loss on frequency at optimum impedance bandwidth.

——— Antenna without Parasitic Element

· · · · · Antenna with Parasitic Element (S = 3.09mm)

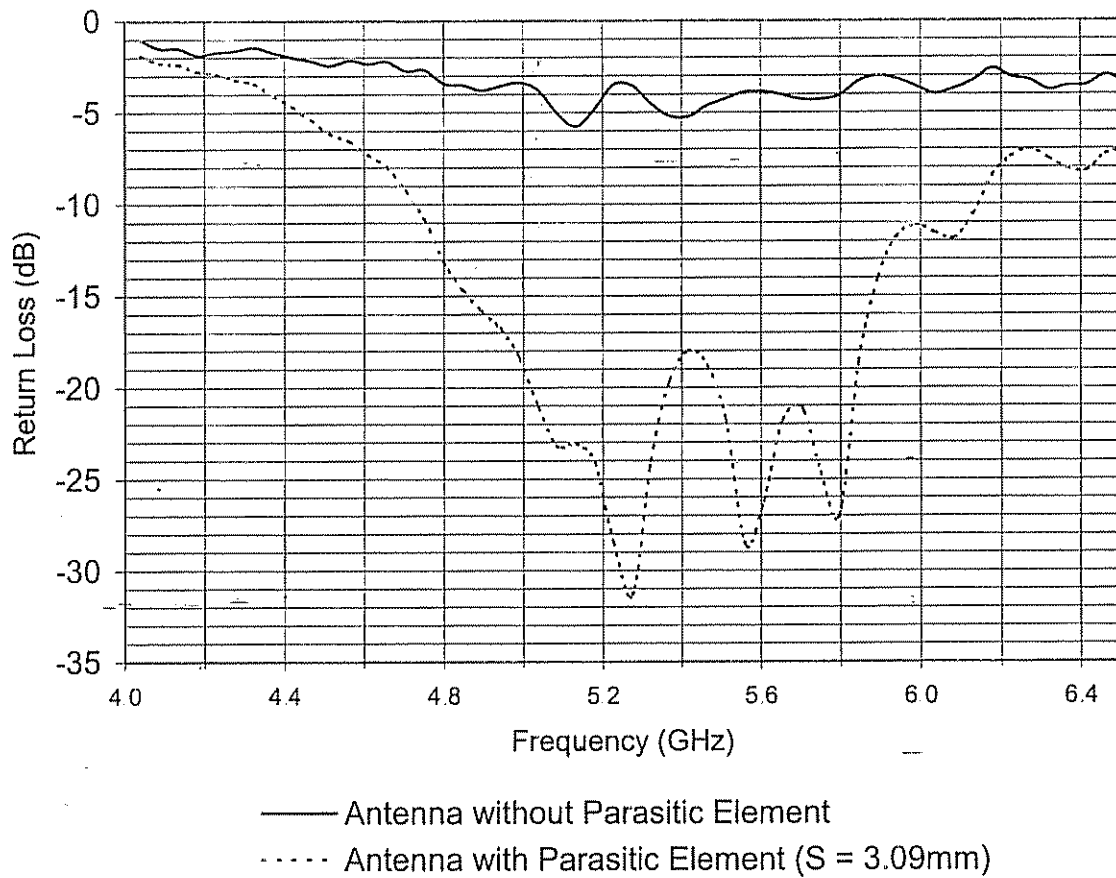Figure 6.7 Experimentally measured return loss versus frequency.

This project also studied the polar pattern of this antenna and figure 6.8 illustrates typical E and H plane radiation patterns calculated at two ends of the frequency band. The corresponding 3 dB beam-widths are:

4.72 GHz:
     E – Plane = 64^0
     H – Plane = 52^0

6.02 GHz:
     E – Plane = 60^0
     H – Plane = 67^0

E-Plane Polar pattern at 4.8 GHz

E-Plane Polar pattern at 5.8 GHz

H-Plane Polar pattern at 4.8 GHz
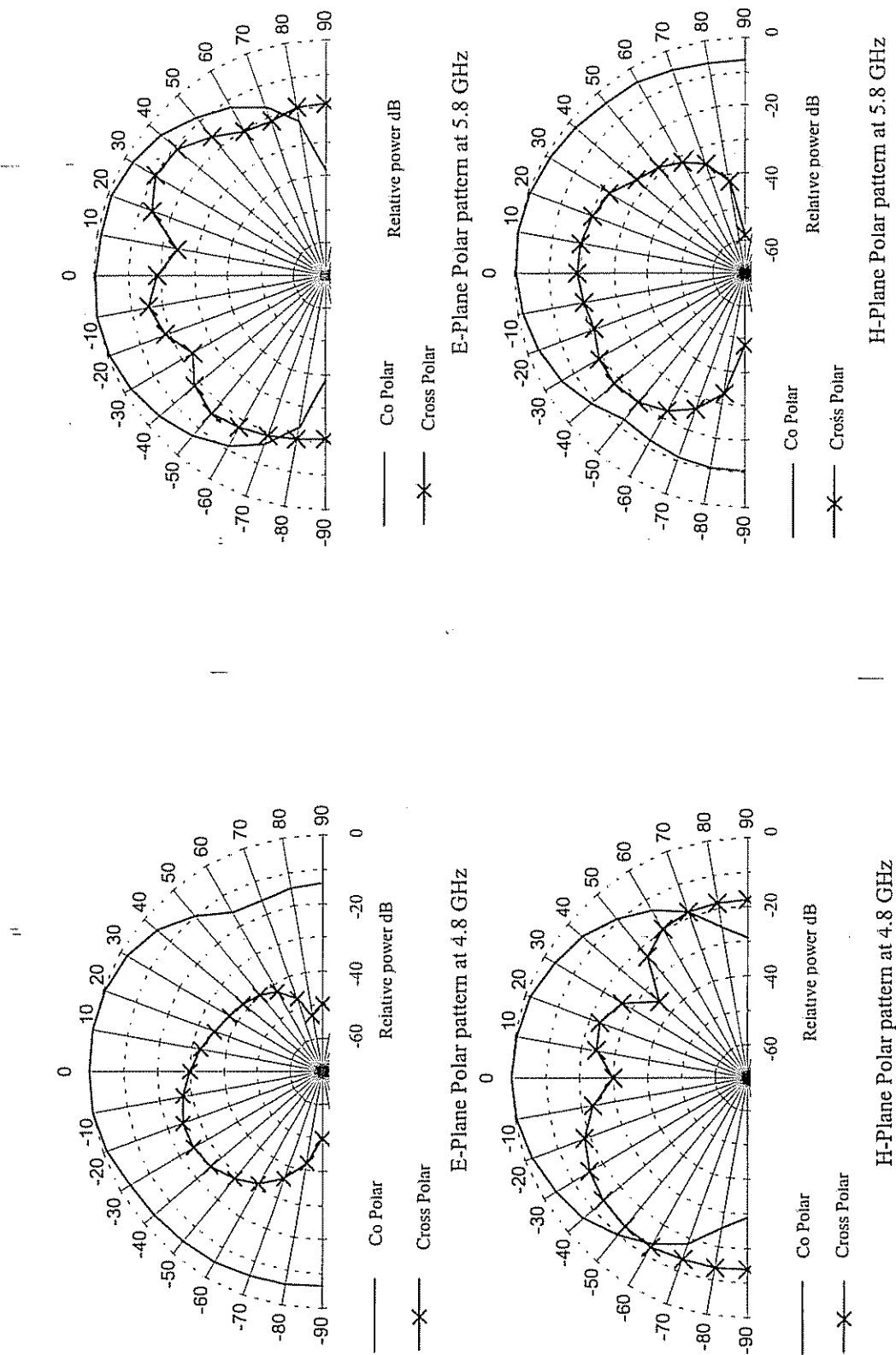
H-Plane Polar pattern at 5.8 GHz

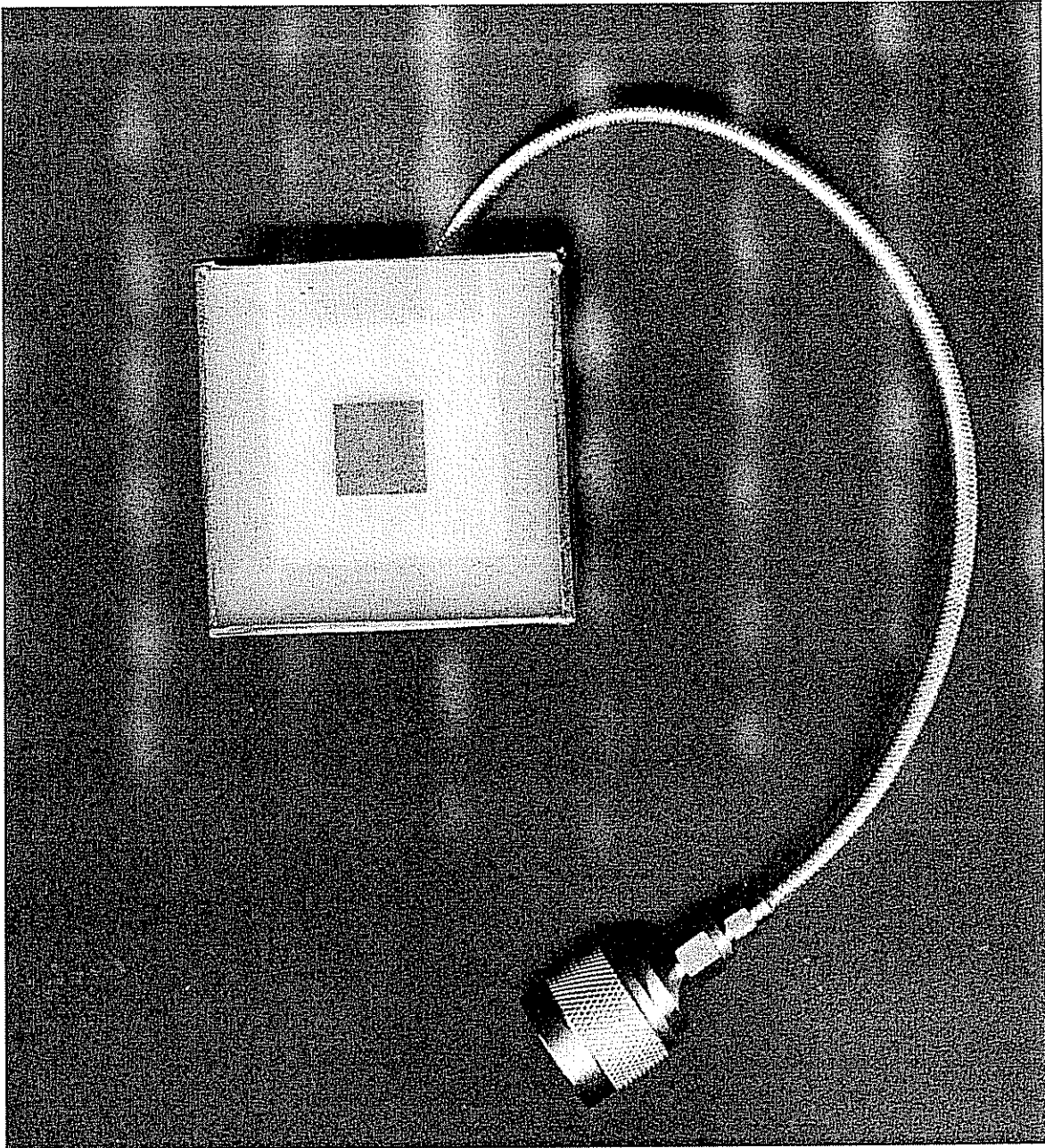Figure 6.8 Radiation patterns at the two ends of frequency band

70

Figure 6.9 The photograph of the actual final antenna

CHAPTER VII

CONCLUSION AND SUGGESTION FOR FUTURE WORKS

7.1 Conclusion

One of the disadvantages of the microstrip patch antenna is its narrow bandwidth. This limitation can be overcome by modifying the conventional microstrip patch antenna. Various methods have been surveyed (chapters two and four) and this lead to the conclusion that no proper design technique has been published yet. All of the published papers and books provide the conceptual design but not the exact technical design steps. This project has studied and proposed a design technique to enhance the antenna bandwidth. This technique has removed the guesswork normally associated with previous wideband microstrip patch antennas design. The method consistently achieved 10-15% antenna bandwidth. This method involves two important design steps as follows;

a) Locating the feeding probe at a location that will give high mismatching between the feeding probe and the driven patch. It has been shown that this location can be determined experimentally or theoretically.

b) Using the parasitic patch of similar outer shape to tune the whole antenna structure over a wider frequency range.

72

The first step basically defines the location of the probe while the second step defines the function of the parasitic patch. This in effect has removed some of the guesswork associated with the previous design techniques.

With it small thickness and flat surface, the final antenna can be embedded into the skin of the vehicle thus provide communication link without deteriorating the aerodynamic properties of the host body. Another attractive feature of the presented antenna lies in its simplicity. It is very simple to manufacture and using commonly available substrate that also cost effective.

7.2   Suggestion For Future Work

The following are some of the research areas that can be investigated further;

1. The effect of superstrates of different heights and dielectric constants can be investigated for the development of new design techniques.

2. The higher TM_{mn} modes and ways of combining them can be investigated for possible bandwidth enhancement.

3. Theoretical investigation can also be made on the proposed simplified cavity model into ways of utilizing it in conjunction with more rigorous methods such as FDTD and spectrum domain analysis.

REFERENCES

[1]   James, J.R., et al., 'Microstrip Antenna, Theory and Design', Peter Peregrinus Ltd., London, 1981

[2]   Brunetti, C. and Curtis, R.W., 'Printed Circuit Techniques', Proc. of The IRE - Wave and Electrons Section, Jan. 1948, pp 121-161.

[3]   Carver, K.R. and Mink, J.W., 'Microstrip Antenna Technology', IEEE Trans.- Antennas and propagation, Vol. AP-29, No. 1, 1981, pp 2-24.

[4]   James, J.R. and Hall, P.S., 'Handbook of Microstrip Antennas', Volume 1 and 2, Peter Peregrinus Ltd., London, 1989.

[5]   Deschamp, G.A. 'Microstrip Microwave Antennas', 3rd USAF Symposium on Antennas, 1953.

[6]   Gutton, H. and Baissinot, G., 'Flat Aerial for Ultra High Frequency', French Patent No. 703113, 1955.

[7]   Lewin, L., 'Radiation from Discontinuities in Stripline', Proc. IEE, Vol. 107c, 1960, pp 163-170.

[8]   Howell, J.Q., 'Microstrip Antennas', IEEE Trans. Antennas and Propagation, Vol. AP-23, No. 1, 1975, pp 90-93.

[9]   Derneryd, A.G., 'Microstrip Disc Antenna', Microwave J, Vol. 21, 1978, pp 77-79.

[10]   Long, S.A. and Walton, M.D., 'A Dual-Frequency Stacked Circular-Disc Antenna', IEEE Trans. Antennas and Propagation, Vol. AP-27, No. 2, 1979, pp 270-273.

[11]   Mcllvenna, J. and Kernweis, N., 'Modified Circular Microstrip Antenna Elements', Electron. Lett., Vol. 15, No. 7, 1979, pp. 2-24.

[12] Schaubert, D.H., Farrar, F.G., Sindoris, A. and Hayes, S. T., 'Microstrip Antennas with Frequency Agility and Polarisation Diversity', IEEE Trans. Antennas and Propagation, Vol. AP-29, No. 1, 1981, pp. 118-123.

[13] Chew, W.C., 'A Broad-Band Annular-Ring Microstrip Antenna', ibid., Vol. AP-30, No. 5, 1982, pp. 918-922.

[14] Garg, R. and Rao, K.V.S., 'Dual Frequency Microstrip Antenna', Electron. Lett., Vol. 19, No. 10, 1983, pp. 357-358.

[15] Ness, J. and Young, R., 'Two-Layer Circularly Polarised Microstrip Antenna', ibid., Vol. 20, No. 4, 1984, pp 181-182.

[16] Fong, K.S., Pues, H.F. and Withers, M.J., Wideband Multilayer Coaxial Fed Microstrip Antenna Element', ibid., Vol. 21, No. 11, 1985, pp 497-498.

[17] Davidson, S.E., Long, S.A. and Richards, W.F., 'Dual Band Reactively Loaded Microstrip Antenna', IEEE Trans. Antenna and Propagation, Vol. AP-33, No. 5, 1985, pp. 556-561.

[18] Davidson, S.E., Long, S.A. and Richards, W.F., 'Dual Band Microstrip Antennas with Monolithic Reactive Loading', Electron. Lett., Vol. 21, No. 20, 1985, pp. 936-937.

[19] Mehler, M.J., Maclean, T.S.N. and Abbas, A.K., 'Input Impedance of a Circular Microstrip Disc Antenna Using Mode Matching', ibid., Vol. 22, No. 7, 1986, pp. 362-363.

[20] Lee, R.Q., Lee, K.F. and Bobinchak, J., 'Characteristics of a Two Layer Electromagnetically Coupled Rectangular Patch Antenna', ibid., Vol. 23, No. 20, 1987, pp. 1070-1072.

[21] Hall, P.S., 'Probe Compensation in Thick Microstrip Patches', ibid., Vol. 23, No. 11, 1987, pp. 606-607.

[22] Smith, H.K. and Mayes, P.E., 'Stacking Resonators to Increase the Bandwidth of Low Profile Antennas', IEEE Trans. Antennas and Propagation, Vol. AP-35, No. 12, 1987, pp. 1473-1476

[23] Wang, J., Fralich, R., Wu, C. and Litva, J., 'Multi Functional Aperture Coupled Stack Patch Antenna', Electron. Lett., Vol. 26, No. 25, 1990, pp. 2067-2068.

[24] Talty, T., Lee, R.Q. and Lee, K.F., 'Circular Polarisation Characteristics of Stacked Microstrip Antennas', ibid., Vol. 26, No. 25, 1990, pp. 2109-2110.

[25] Lee, C.S. and Nalbandian, V., 'Impedance Matching of a Dual Frequency Microstrip Antenna with an Air Gap', IEEE Trans. Antennas and Propagation, Vol. AP-41, No. 5, 1993, pp. 680-682.

[26] Itoh, T. and Mittra, R, 'Spectral Domain Approach for Calculating the Dispersion Characteristic of Microstrip Lines', IEEE Trans. on MTT, Vol. MTT-21, No. 7, 1973, pp 496-499.

[27] Itoh, T., 'Analysis of Microstrip Resonators', ibid., Vol. MTT-22, No. 11, 1974, pp 946-952.

[28] Harrington, R.F., 'Field Computation by Method of Moments', MacMillan, New York, 1968.

[29] Munson, R.E., 'Conformal Microstrip Antennas and Microstrip Phase Arrays', IEEE Trans. Antenna and Propagation, Vol. AP-22, No. 1, 1974, pp 74-78.

[30] Derneryd, A.G., 'Linearly Polarised Microstrip Antenna', ibid., Vol. AP-24, No. 6, 1976, pp 846-851.

[31] Lo, Y.T., Harrison, D.D., Solomon, D., Deschamps, G.A. and Ore, F.R., 'Study of Microstrip Antennas, Microstrip Phased Arrays and Microstrip Feed Networks', Rome Air Development Centre, Tech. Report TR-77-406, 1977.

[32] Itoh, T. and Menzel, W. 'A Full Wave Analysis Method for Open Microstrip Structures', IEEE Trans. Antennas and Propagation, Vol. AP-29, No. 1, 1981, pp 63-68.

[33] Rana, I.E. and Alexopoulos, N.G., 'Current Distribution and Input Impedance of Printed Dipoles', ibid., Vol. AP-29, No. 1, 1981, pp 99-105.

[34] Sommerfeld, A., 'Partial Differential Equation in Physic', Academic Press Inc., 1949.

[35] Pozar, D.M., 'Input Impedance and Mutual Coupling of Rectangular Microstrip Antennas', IEEE Trans. Antennas and Propagation, Vol. AP-30, No. 6, 1982, pp 1191-1196.

[36] Desphande, M.D. and Bailey, M.C., 'Input Impedance Microstrip Antennas', ibid., Vol. AP-30, No. 4, 1982, pp 645-650.

[37] Desphande, M.D. and Bailey, M.C., 'Integral Equation Formulation of Microstrip Antenna', ibid., Vol. AP-30, No. 4, 1982, pp 651-656.

[38] Mosig, J.R. and Gardiol, F.E., 'A Dynamic Radiation Model for Microstrip Structure', In Hawkes, D. (Ed): Advance in Electronics and Electron Physics, Academic Press Inc., New York, 1982, pp 139-237.

[39] Van, L. and De Capelle, V., 'Transmission Line Model for Mutual Coupling Between Microstrip Antennas', IEEE Trans. Antennas and Propagation, Vol. AP-32, No. 8, 1984, pp 816-821.

[40] Bailey, M.C. and Deshpande, M.D., 'Analysis of Rectangular Microstrip Antennas', NASA Technical Paper 2276, 1984.

[41] Lan, G.I. and Sengupta, D.L., 'Tunable Circular Patch Antennas', Electronics Lett., No. 22, 1985, pp 1022-1023.

[42] Mosig, J.R. and Gardiol, F.E., 'General Integral Equation Formulation for Microstrip Antennas and Scatterers', IEE Proc.-H (Microwaves, Antenna and Propagation), Vol. 132, No. 7, 1985, pp 424-432.

[43] Araki, K., Ueda, H. and Masayaki, T., 'Numerical Analysis for Circular Disk Microstrip Antennas with Parasitic Elements', IEEE Trans. Antennas and Propagation, Vol. AP-34, No. 12, 1986, pp 1390-1394.

[44] Uzunoglu, N.K., Alexopoulos, N.G. and Fikioris, J. G., 'Radiation Properties of Microstrip Dipoles', ibid., Vol. AP-27, 1979, pp 853-858.

[45] Toland, B., Lin, J., Houshmand, B. and Itoh, T., 'FDTD Analysis on an Active Antenna', IEEE Microwave and Guided Wave Letters, Vol. 3, No. 11, 1993, pp 423-425.

[46] Proust, I., Sauviac, B., Amalnic, J.L. and Baudrand, H., 'Influence of Feed Probes on Input Impedance and Performance of Patch Antennas', 23rd European Microwave Conference Proceedings, Spain, Sept. 1993, Vol. 1, pp 926-928.

[47] Eswarappa, C. and Heofer, W.J.R., 'Absorbing Boundary for 3D-TLM Modelling of Microstrip Patch Antennas', 23rd European Microwave Conference Proceeding, Spain, Sept. 1993, Vol. 1, pp 291-292.

[48] Higdon, R.L., 'Numerical Absorbing Boundary Conditions for the Wave Equation', Math. Comp., Vol. 49, No. 179, July 1987, pp 65-91.

[49] Vechinski, D.A., Rao, S.M. and Sarkar, T.K., 'Time Domain Integral Equation Method Applied to Antenna Problems', 23rd European Microwave Conference Proceeding, Spain, Sept. 1993, Vol. 1, pp 34-35.

[50] Shively, D.G. and Bailey, M.C., 'Analysis of Microstrip Patch Antennas With Nonzero Surface Resistance', NASA Technical Paper 3362, Cecom Technical Report 93-E-2, 1993

[51] Hassani, H.R. and Mirshekar-Syahkal, D., 'Study of Electromagnetically Coupled Stacked Rectangular Patch Antennas', IEE Proc.-H (Microwaves, Antennas and Propagation), Vol. 142, No. 1, 1995, pp 7-13.

[52] Chebolu, S., Mittral, R. and Becker, W.D., 'The analysis of Microwave Antennas Using the FDTD Method', Microwave J., Jan. 1996, pp 134-150.

[53] Stephen, K.D. and Young, S., 'Mode Stability of Radiation-Coupled Inter-Injection-Locked Oscillator for Integrated Phase Array', ibid., Vol. MTT-36, No. 5, 1988, pp 921-924

[54] Chang. K.; Hummer, K.A. and Gopalakrishnan, G.K., 'Active Radiating Element Using FET Source Integrated with Microstrip Patch Antenna', Electron. Lett., Vol. 24, No. 21, 1988, pp 1347-1348.

[55] Yee, K.S., 'Numerical Solution of Initial Boundary Value Problems Involving Maxwell's Equations in Isotropic Media', IEEE Trans. Antenna and Propagation, May 1964.

[56] Hilton, G.S.,Railton, C.J. and Beach, M.A., 'Modelling Parasitically Coupled Patch Antenna Using The Finite Difference Time Domain Technique', 8th International Conference on Antennas and Propagation, Part 1, IEE Conference Publication No. 370, 1993.

[57] Chebolu, S. and Mittra, R. 'The Analysis of Microwave Antennas Using The FDTD Method', Microwave J. Vol. 39, No. 1, January 1996.

[58] Sanchez-Hernandez, D. and Robertson, I.D., 'A Survey of broadband Microstrip Patch Antennas', Microwave J., Sept. 1996, pp 60-84.

[59] Carlin, H.J. and Komiak, J.J., 'A New Method of Broadband Equalisation Applied to Microwave Amplifier', IEEE Trans. Microwave Theory and Technique, Vol. MTT-27, No. 2, 1979, pp 93-99.

[60] Pues, H.F. and Van de Capelle, A.R., 'An Impedance-Matching Technique for Increasing the Bandwidth of Microstrip Antennas', IEEE Trans. Antennas and Propagation, Vol. AP-37, No. 11, 1989, pp. 1345-1354.

[61] An, H., Nauwelaers, B.K.J.C., Van de Capelle, A.R., 'Broadband Microstrip Antenna Design with Simplified Real Frequency Technique', ibid., Vol. AP-42, No. 2 1994, pp 129-136.

[62] Long, S.A. and Walton, M.D., 'A Dual-Frequency, Stacked Circular Disc Antenna', IEEE Antennas and Propagation Society International Symposium, 1978 Digest, Vol. 1, pp 260-263.

[63] Heberling, D., 'Simple Feeding Technology for Stacked Microstrip Antennas', 19th European Microwave Conference Digest, London, UK, September 1989, pp 155-160.

[64] Cock, R.T. and Christodoulu, C.G., 'Design of a Two-Layer, Capacitively Coupled, Microstrip Patch Antenna Element for Broadband Applications', IEEE Antennas and Propagation Society International Symposium, 1987 Digest, Vol. 2, pp 936-939.

[65] Croq, F., 'Stacked Resonators for Bandwidth Enhancement: A Comparison of Two Feeding Techniques', IEE Proceedings, Part H, Vol. 140, No. 4, 1993, pp 303-309.

[66] Damians, J.P., 'Study of Multilayer Microstrip Antennas with Radiating Elements of Various Geometry', IEE Proceedings, Part H, Vol. 137, No. 3, 1990, pp 163-170.

[67] Damians, J.P., ' Dual-Frequency and Offset Multilayer Microstrip Antennae', 8th IEE International Conference on Antennas and Propagation, Heriot-Watt University, U.K., 1993, pp. 732-735

[68] Mittra, R., 'Microstrip Patch Antennas for GPS Applications', IEEE Antennas and Propagation Society International Symposium, 1993 Digest, Vol. 3, pp. 1478-1481.

[69] Dahele, J.S. and Lee, K.F., 'Characteristics of Annular-Ring Microstrip Antennas', Electronic Lett., Vol. 18, No. 24, 1982, pp 1051-1052.

[70] Lee, K.F., Ho, K.Y. and Dahele, J.S., 'Circular-Disk Microstrip Antenna With an Airgap', IEEE Trans. Antennas and Propagation, Vol. AP-32, No. 8, 1984, pp 880-884.

[71] Dahele, J.S., Tung, S.H. and Lee, K.F., 'Normal and Inverted Configuration of the Broadband Electromagnetically-Coupled Microstrip Antennas', IEEE Antennas

and Propagation Society International Symposium, 1986 Digest, Vol. 2, pp 841-844.

[72] Chen, C.H., Tulinfsetf, A. and Sorbello, R.M., 'Broadband Two Layer Microstrip Antenna', IEEE Antennas and Propagation Society International Symposium, 1984 Digest, Vol. 1, pp. 251-254.

[73] Pues, H., Vandensande, J., Van de Capelle, A. and Leuven, K.U., 'Broadband Microstrip Resonator antennas', IEEE Antenna and Propagation Society International Symposium, 1978 Digest, pp 1478-1481.

[74] Kumar, G. and Gupta, K.C., 'Broadband Microstrip Antennas Using Additional Resonators Gap Coupled to the Radiating Edges', IEEE Trans. Antennas and Propagation, Vol. AP-32, No. 12, 1984, pp 1375-1379.

[75] Kumar, G. and Gupta, K.C., 'Nonradiating Edges and Four Edges Gap Coupled Multiple Resonator Broadband Microstrip Antennas', bid, Vol. AP-33, No. 2, 1985, pp 173-178.

[76] Chang, D.C. and Zheng, J.X., 'A Wideband Microstrip Antenna Using Two Triangular Patches', IEEE Antenna and Propagation Society International Symposium, 1991 Digest, Vol. 1, pp 72-75.

[77] Ketineni, R.V., Balaji, Uma and Das A. 'Improvement of Bandwidth in Microstrip Antennas Using Parasitic Patch', IEEE Antennas and Propagation Society International Symposium, 1992 Digest, Vol. 3, pp 1943-1947.

[78] Hall, P.S., 'New Wideband Microstrip Antenna Using Log-Periodic Technique', Electronic Lett., Vol. 16, No. 4, 1980, pp 127-128.

[79] Pues, H.,Bogaers, J., Pieck, R. and Van de Capelle, A., 'Wideband Quasi-Log-Periodic Microstrip Antenna', IEE Proceeding Part H, Vol. 128, No. 3, 1981, pp 159-163.

[80] Hoorfar, A. and Chang, K.C., 'A Novel Log-Periodic Microstrip Array', URSI International Symposium, 1990 Digest, p. 16.

[81] Du Plessis, M. and Cloete, J,H., 'Tuning Stubs for Microstrip Patch Antennas', IEEE Antennas and Propagation Society International Symposium, 1993 Digest, Vol. 2, pp. 964-967.

[82] Pozar, D.M., 'Trimming Stubs for Microstrip Feed Networks and Patch Antennas', IEEE Antennas and Propagation Society Newsletter, December 1987, pp 26-28.

[83] Richards, W.F., Davidson, S.E. and Long, S.A, 'Dual-Band Reactively Loaded Microstrip Antenna', IEEE Trans. Antennas and Propagation, Vol. AP-33, No. 5, 1985, pp. 556-561.

[84] Al-Charchafchi, S.H. and Kyriopoulos, J., 'A Varactor Tuned Microstrip Patch Antenna', IEE International Conference on Antennas and Propagation, Conference Publication No. 407, 1995, pp. 278-281.

[85] Glatz, P., Daryoush, A.S. and Herczfeld, P.R., 'Theoretical and Experimental Analysis of Optically Tuned Patch Antenna', IEEE Antennas and Propagation Society International Symposium, 1987 Digest, Vol. 1, pp 439-442.

[86] Schaubert, D.H., Farrar, F.G., Sindoris, A and Hayes, S.T., 'Microstrip antennas with Frequency Agility and Polarisation Diversity', IEEE Trans. Antennas and Propagation, Vol. AP-29, No.1, 1981 pp 118-123

[87] Dey, S., 'A New Circular Patch Antenna', IEEE Antennas and Propagation Society International Symposium, 1993 Digest, Vol. 2, pp 976-979.

[88] Compton, R.C., McPhedran, R.C., Popovic, Z., Rebeiz, G.M., Tong, P.P. and Rutledge, D.B., 'Bow-Tie Antennas on a dielectric Half Space: Theory and Experiment', IEEE Trans. on Antennas and Propagation, Vol. AP-35, No. 6, 1987, pp 622-631.

[89] Dubost, G., 'Flat Radiating Dipoles and Application to Arrays', John Wiley & Son, Research Studies Press, pp. 24-28.

[90] Poddar, D.R., Chatterjee, J.S. and Chowdhury, S.K., 'On Some Broadband Microstrip Resonators', IEEE Trans. Antennas and Propagation, Vol. AP-31, No. 1, 1983, pp 193-194.

[91] Hall, P.S., Wood, C. and Garrett, C., 'Wide Bandwidth Microstrip Antennas for Circuit Integration', Electronics Lett., Vol. 15, No. 15, 1979, pp 458-459.